

ASC Report No. 40/2011

# **A high frequency hp boundary element method for scattering by convex polygons**

D.P. Hewett, S. Langdon, J.M. Melenk

Institute for Analysis and Scientific Computing  
Vienna University of Technology — TU Wien  
[www.asc.tuwien.ac.at](http://www.asc.tuwien.ac.at) ISBN 978-3-902627-04-9

## Most recent ASC Reports

- 39/2011 *A. Jüngel*  
Semiconductor Device Problems
- 38/2011 *L. Neumann, A. Arnold, W. Hochhauser*  
Zur Stabilität von geklebten und geklotzten Glasscheiben: Beurteilung der Dunkerley'schen Geraden zur Beulwertbestimmung
- 37/2011 *A. Dick, O. Koch, R. März, E. Weinmüller*  
Collocation Schemes for Nonlinear Index 1 DAEs with a Singular Point
- 36/2011 *J.A. Carrillo, S. Hittmeir, A. Jüngel*  
Cross diffusion and nonlinear diffusion preventing blow up in the Keller-Segel model
- 35/2011 *P. Fuchs, A. Jüngel, M. von Renesse*  
On the Lagrangian structure of quantum fluid models
- 34/2011 *W. Auzinger, O. Koch, M. Thalhammer*  
Defect-based local error estimators for splitting methods, with application to Schrödinger equations Part I. The linear case
- 33/2011 *A. Jüngel, R. Weishäupl*  
Blow-up in two-component nonlinear Schrödinger systems with an external driven field
- 32/2011 *S. Ferraz-Leite, JM. Melenk, D. Praetorius*  
Numerical quadratic energy minimization bound to convex constraints in thin-film micromagnetics
- 31/2011 *JM. Melenk, C. Xenophontos, L. Oberbroeckling*  
Robust exponential convergence of hp-FEM for singularly perturbed reaction diffusion systems with multiple scales
- 30/2011 *JM. Melenk, C. Xenophontos, L. Oberbroeckling*  
Analytic regularity for a singularly perturbed system of reaction-diffusion equations with multiple scales: a rood map

Institute for Analysis and Scientific Computing  
Vienna University of Technology  
Wiedner Hauptstraße 8–10  
1040 Wien, Austria

**E-Mail:** [admin@asc.tuwien.ac.at](mailto:admin@asc.tuwien.ac.at)  
**WWW:** <http://www.asc.tuwien.ac.at>  
**FAX:** +43-1-58801-10196

ISBN 978-3-902627-04-9

© Alle Rechte vorbehalten. Nachdruck nur mit Genehmigung des Autors.



# A HIGH FREQUENCY $hp$ BOUNDARY ELEMENT METHOD FOR SCATTERING BY CONVEX POLYGONS

D. P. HEWETT\*, S. LANGDON\*, J. M. MELENK†

**Abstract.** In this paper we propose and analyse a hybrid  $hp$  boundary element method for the solution of problems of high frequency acoustic scattering by sound-soft convex polygons, in which the approximation space is enriched with oscillatory basis functions which efficiently capture the high frequency asymptotics of the solution. We demonstrate, both theoretically and via numerical examples, exponential convergence with respect to the order of the polynomials, moreover providing rigorous error estimates for our approximations to the solution and to the far field pattern, in which the dependence on the frequency of all constants is explicit. Importantly, these estimates prove that, to achieve any desired accuracy in the computation of these quantities, it is sufficient to increase the number of degrees of freedom in proportion to the logarithm of the frequency as the frequency increases, in contrast to the at least linear growth required by conventional methods.

**Key words.** High frequency scattering, Boundary Element Method,  $hp$ -method

**AMS subject classifications.** 65N12, 65N38, 65R20

**1. Introduction.** Conventional numerical schemes for time-harmonic acoustic scattering problems, with piecewise polynomial approximation spaces, become prohibitively expensive in the high frequency regime where the scatterer is large compared to the wavelength of the incident wave. For two-dimensional problems the number of degrees of freedom required to achieve a prescribed level of accuracy grows at least linearly with respect to frequency. On the other hand, approximation via high frequency asymptotics alone is often insufficiently accurate when the frequency lies within ranges of practical interest. These issues are very well understood; see e.g. [9, 10, 37, 30, 12] and the many references therein.

The problem of ‘bridging the gap’ between conventional numerical methods and fully asymptotic approaches has received a great deal of attention in recent years. Significant progress has been made in developing numerical methods which can achieve a prescribed level of accuracy at high frequencies with fewer degrees of freedom than conventional approaches. A key idea underpinning much recent work is to express the scattered field as a sum of products of known oscillatory functions, selected using knowledge of the high frequency asymptotics, with slowly oscillating amplitude functions, and to approximate just the amplitudes by piecewise polynomials (we call this the *hybrid numerical-asymptotic approach*). Applying this idea within a boundary element method (BEM) context is particularly attractive since in this case one need only understand the high frequency behaviour on the boundary of the scatterer, rather than throughout the whole propagation domain. Computational methods implementing this approach have been applied successfully to problems of scattering by both smooth [8, 21, 22, 26] and non-smooth [15, 20, 2, 29, 16] convex scatterers, the latter building on previous work on hybrid  $h$ -version BEM methods for the special problem of acoustic scattering in a half-space with impedance boundary conditions [28].

In this paper we propose an  $hp$ -version BEM for high frequency scattering by sound-soft convex polygons based on this hybrid numerical-asymptotic approach, and

---

\*Department of Mathematics and Statistics, University of Reading, Whiteknights PO Box 220, Reading RG6 6AX, UK, email: d.p.hewett@reading.ac.uk, s.langdon@reading.ac.uk. Supported by EPSRC grant EP/F067798/1

†Institut für Analysis und Scientific Computing, TU Wien, A-1040 Wien, Austria, email: melenk@tuwien.ac.at

we study its properties and performance by numerical experiments backed up by rigorous numerical analysis. We show that our algorithm is exponentially convergent as a function of  $\sqrt{N}$ , where  $N$  is the number of degrees of freedom, for fixed wavenumber  $k$  ( $k = 2\pi f/c$  where  $f$  is the frequency and  $c$  the wave speed). More importantly (and it is for this property that the hybrid approach is key) our algorithm provably achieves any desired accuracy, uniformly over all wave numbers  $k$ , provided  $N$  increases logarithmically with  $k$ . These results improve on the  $h$ -version Galerkin BEM for the identical problem in [15], which is only algebraically convergent, and we note that the most sophisticated algorithm to date [21] for smooth 2D convex obstacles, while accurate for  $N$  and  $k$  large, is not convergent as  $N \rightarrow \infty$  for  $k$  fixed.

Our results go beyond those of previous authors in terms of analysis in a number of important respects. Firstly, these are the first numerical analysis results for a hybrid approach which make explicit the dependence of all constants in the error estimates on the wavenumber  $k$  and both the  $h$  and  $p$  discretisation parameters. Secondly, this is the first numerical analysis for a bounded obstacle scattering problem which establishes that it is sufficient to increase  $N$  proportional to powers of  $\log k$  to maintain accuracy as  $k \rightarrow \infty$ . The best previous result for smooth convex obstacles ([43], refining results in [21]) establishes that it is sufficient to increase  $k$  slightly faster than  $k^{1/9}$  to retain accuracy, while the analysis in [15], when completed by the coercivity estimates of [43] and the estimates in §4 below, also requires a mild algebraic growth in  $N$  as  $k \rightarrow \infty$  to maintain accuracy. (We note however that the hybrid  $h$ -version BEM proposed in [28], for the special problem of scattering in a half-plane with impedance boundary conditions, is shown in [28] to achieve any required accuracy uniformly in the wavenumber with  $N$  independent of  $k$ .)

We note that the  $hp$ -BEM we describe in this paper was briefly sketched in [36]; in this paper we describe the method in detail, provide a rigorous derivation of error estimates in the Galerkin solution, and demonstrate that our theoretical estimates are achieved by the BEM in practice. We also demonstrate theoretically and numerically how the error in the BEM solution depends on the scatterer geometry. Our method is based on the fact that on the boundary  $\Gamma$  of the polygon the normal derivative of the solution  $u$  to the scattering problem can be decomposed as

$$\frac{\partial u}{\partial \mathbf{n}}(\mathbf{x}(s)) = \Psi(\mathbf{x}(s)) + v^+(s)e^{iks} + v^-(s)e^{-iks}, \quad (1.1)$$

where  $\mathbf{x}(s)$  represents a point on  $\Gamma$ ,  $s \in [0, L]$  represents arc length around  $\Gamma$  and  $L$  is the length of  $\Gamma$ . In (1.1), the leading order term  $\Psi$  represents the so-called ‘‘Physical Optics’’ approximation to  $\partial u/\partial \mathbf{n}$ ; explicitly,  $\Psi := 2\partial u^i/\partial \mathbf{n}$  on the sides of the polygon illuminated by the incident wave  $u^i$  (which is assumed to be a plane wave), and  $\Psi := 0$  on the shadow sides. The second and third terms in (1.1) represent diffracted waves propagating around the boundary in opposite directions. It was shown in [15], via bounds on derivatives of  $v^\pm(s)$  for  $0 \leq s \leq L$ , that the coefficients  $v^\pm(s)$  are slowly-varying, except in the vicinity of the corners of the polygon where they are singular. Accordingly, they can be approximated by piecewise polynomials much more efficiently than can  $\partial u/\partial \mathbf{n}$ , and this is the basis on which our  $hp$  approximation space is designed. In this paper we extend these results significantly, showing that  $v^\pm(s)$  have analytic continuations into the complex  $s$ -plane, whose absolute values can be bounded explicitly in terms of  $k$  and the distance from the corner singularities. This result plays a large part in our  $hp$  approximation theory, but is of interest in its own right as a result in high frequency asymptotics and for the analysis of other numerical schemes; for example it may be that this result provides tools necessary to analyse

boundary integral equation based numerical methods which use quadrature rules that require the path of integration to be deformed into the complex plane (e.g. [26, 3]).

Our analyticity assertions for the slowly-varying parts  $v^\pm(s)$  permit us to show exponential convergence for the approximation by piecewise polynomial approximations on geometrically refined meshes. The reasons for the success of the geometric mesh idea in the present hybrid  $hp$ -BEM are the same as those leading to the well-known exponential convergence of the classical  $hp$ -FEM [23, 24, 5, 42, 41] and  $hp$ -BEM [4, 45, 32, 25] for elliptic problems in corner domains, namely, the analyticity of the function to be approximated in conjunction with explicit control over how higher order derivatives blow up as the singularity is approached.

This paper concentrates on the approximation theory of our scheme. Practical implementation issues are addressed in [35], where in particular the question of how to compute the stiffness matrix with a computational cost that depends only very mildly on the frequency is considered in some detail. Compared to the classical  $hp$ -BEM, highly oscillatory integrals have to be evaluated that arise from both the kernels of the integral operators and the hybrid ansatz. This quadrature issue therefore differentiates the present hybrid  $hp$ -BEM from the classical  $hp$ -BEM, for which the quadrature is understood to a significant extent, [39, 40].

An outline of the paper is as follows. In §2 we state precisely the scattering problem to be solved, and review some key recent results relating to the reformulation of the problem as a boundary integral equation (BIE). In §3 we derive regularity estimates for the solution of the BIE. These estimates involve the supremum of the total field in the domain; in §4 we prove a frequency-explicit bound on this quantity. In §5 we define our  $hp$  approximation space, and derive rigorous best approximation error estimates for the solution of the BIE. In §6 we describe our Galerkin method, and prove error estimates for the Galerkin approximation to the solution of the boundary integral equation, for the approximation to the resulting solution in the domain and for the approximation to the far field pattern. Numerical results are presented in §7.

In our implementation and analysis we focus on sound-soft convex polygons. Essentially the same numerical method extends to convex polygons with other boundary conditions, e.g. Neumann, impedance. Further, much of the analysis, in particular our regularity and best approximation results should be extendable to that case, and our  $hp$  algorithms are also potentially adaptable to curvilinear polygons (see [16, 29] for  $h$ -version results in these directions). More challenging is any extension to non-convex polygons: see [14, 13]. With possible extensions to non-convex scatterers in mind, some of the results in the current paper, in §2 and §4 in particular, are stated and proved in more generality than is required for the convex case.

**2. Problem Statement.** We consider the two-dimensional problem of scattering of a time-harmonic incident plane wave by a sound-soft polygon. Let  $\Omega \subset \mathbb{R}^2$  denote the interior of the scatterer and  $D := \mathbb{R}^2 \setminus \overline{\Omega}$  the unbounded exterior domain. The boundary value problem (BVP) we wish to solve is: given the incident field

$$u^i(\mathbf{x}) := e^{ik\mathbf{x}\cdot\mathbf{d}}, \quad (2.1)$$

where  $k > 0$  is the wavenumber,  $\mathbf{x} = (x_1, x_2) \in \mathbb{R}^2$ , and  $\mathbf{d}$  is a unit direction vector, determine the total field  $u \in C^2(D) \cap C(\overline{D})$  such that

$$\begin{aligned} \Delta u + k^2 u &= 0, & \text{in } D, \\ u &= 0, & \text{on } \Gamma := \partial\Omega, \end{aligned} \quad (2.2)$$

and  $u^s := u - u^i$  satisfies the Sommerfeld radiation condition. It follows from standard arguments connecting formulations in classical function spaces to those in a Sobolev space setting (see e.g. [18, Theorem 3.7]) that if  $u$  satisfies the above BVP then also  $u \in H_{\text{loc}}^1(D)$ , and, from standard elliptic regularity results, it follows moreover that  $u$  is  $C^\infty$  up to the boundary of  $\partial D$ , excluding the corners of the polygon.

Next we state our integral equation formulation. From [33, Theorems 7.15 and 9.6], for details see [15], we observe that if  $u$  satisfies the BVP then a form of Green's representation theorem holds, namely

$$u(\mathbf{x}) = u^i(\mathbf{x}) - \int_{\Gamma} \Phi_k(\mathbf{x}, \mathbf{y}) \frac{\partial u}{\partial \mathbf{n}}(\mathbf{y}) \, ds(\mathbf{y}), \quad \mathbf{x} \in D, \quad (2.3)$$

where  $\Phi_k(\mathbf{x}, \mathbf{y}) := (i/4)H_0^{(1)}(k|\mathbf{x} - \mathbf{y}|)$  is the fundamental solution for (2.2) and  $\partial u / \partial \mathbf{n} \in L^2(\Gamma)$ , with  $\mathbf{n}$  the unit normal directed into  $D$ . Furthermore, the BVP can be reformulated as a BIE for  $\partial u / \partial \mathbf{n} \in L^2(\Gamma)$ , taking the form

$$\mathcal{A} \frac{\partial u}{\partial \mathbf{n}} = f, \quad (2.4)$$

where  $f \in L^2(\Gamma)$  and  $\mathcal{A} : L^2(\Gamma) \rightarrow L^2(\Gamma)$  are specified next.

**Classical combined potential formulation.** In the standard combined potential formulation (e.g. [19]),

$$\mathcal{A} = \mathcal{A}_{k,\eta} := \frac{1}{2}\mathcal{I} + \mathcal{D}'_k - i\eta\mathcal{S}_k,$$

and  $f = \partial u^i / \partial \mathbf{n} - i\eta u^i$ , where  $\mathcal{I}$  is the identity operator,

$$\mathcal{S}_k \psi(\mathbf{x}) := \int_{\Gamma} \Phi_k(\mathbf{x}, \mathbf{y}) \psi(\mathbf{y}) \, ds(\mathbf{y}), \quad \mathbf{x} \in \Gamma, \quad \psi \in L^2(\Gamma),$$

is the single-layer potential,

$$\mathcal{D}'_k \psi(\mathbf{x}) := \int_{\Gamma} \frac{\partial \Phi_k(\mathbf{x}, \mathbf{y})}{\partial \mathbf{n}(\mathbf{x})} \psi(\mathbf{y}) \, ds(\mathbf{y}), \quad \mathbf{x} \in \Gamma, \quad \psi \in L^2(\Gamma),$$

is the adjoint of the double-layer potential and  $\eta$  is a coupling parameter. From the results in [15] for general Lipschitz domains we know that  $\mathcal{A}_{k,\eta}$  is invertible, and hence the BIE (2.4) is uniquely solvable, for all  $k > 0$  provided  $\eta \in \mathbb{R} \setminus \{0\}$ . Recent results ([11, (6.10)], [6, Theorem 2.11]) suggest that, for  $k \text{ diam } \Omega > 1$ , a good choice (in the sense of trying to minimise the condition number of  $\mathcal{A}_{k,\eta}$  and its boundary element discretization) is  $\eta = k$ .

**Star-combined formulation.** Recently [43] a new formulation has been derived for the case when  $\Omega$  is star-like with respect to the origin. This takes the form (2.4) with

$$\mathcal{A} = \mathcal{A}_k := (\mathbf{x} \cdot \mathbf{n}) \left( \frac{1}{2}\mathcal{I} + \mathcal{D}'_k \right) + \mathbf{x} \cdot \nabla_{\Gamma} \mathcal{S}_k - i\hat{\eta} \mathcal{S}_k, \quad (2.5)$$

the so-called ‘‘star-combined’’ potential operator, and  $f(\mathbf{x}) = \mathbf{x} \cdot \nabla u^i(\mathbf{x}) - i\hat{\eta} u^i(\mathbf{x})$ . Here  $\nabla_{\Gamma}$  is the surface gradient operator. From [43] we know that (for  $\Omega$  Lipschitz and star-like)  $\mathcal{A}_k$  is invertible for all  $k > 0$  provided the choice  $\hat{\eta} = k|\mathbf{x}| + i/2$  is made. We assume henceforth this choice of  $\hat{\eta}$  in (2.5), and thus write the star-combined potential operator as  $\mathcal{A}_k$ , with no  $\hat{\eta}$  subscript, to differentiate it from the standard combined potential operator  $\mathcal{A}_{k,\eta}$ .

**Properties of the boundary integral operators.** For both formulations the following lemma holds provided  $\Omega$  is Lipschitz and  $|\eta| \leq Ck$  for the standard formulation. Here and for the remainder of this paper  $C > 0$  denotes a constant whose value may change from one occurrence to the next, but which is always independent of  $k$ , although it may (possibly) be dependent on the geometry of  $\Gamma$ . We use  $C_j, c_j, k_j$ , etc., for  $j = 0, 1, 2, \dots$ , to denote specific constants whose value remains the same throughout the paper.

LEMMA 2.1 ([11, Theorem 3.6], [43, Theorem 4.2]). *Assume that  $\Omega$  is a bounded Lipschitz domain and  $k_0 > 0$ . For the case  $\mathcal{A} = \mathcal{A}_{k,\eta}$  assume additionally  $|\eta| \leq Ck$ . Then for both  $\mathcal{A} = \mathcal{A}_k$  and  $\mathcal{A} = \mathcal{A}_{k,\eta}$  there exists a constant  $C_0 > 0$ , independent of  $k$ , such that*

$$\|\mathcal{A}\|_{L^2(\Gamma)} \leq C_0 k^{1/2}, \quad k \geq k_0.$$

For the case that  $\Omega$  is also star-like, we have the following result:

LEMMA 2.2 ([17, Theorem 4.3], [43]). *If  $\Omega$  is Lipschitz and star-like then, for all  $k_1 > 0$ , there exists a constant  $C_1 > 0$ , independent of  $k$ , such that*

$$\|\mathcal{A}^{-1}\|_{L^2(\Gamma)} \leq C_1, \quad k \geq k_1, \quad (2.6)$$

for both  $\mathcal{A} = \mathcal{A}_k$  and  $\mathcal{A} = \mathcal{A}_{k,\eta}$ , with  $\eta = k$ .

In certain cases  $\mathcal{A}$  also satisfies the following assumption:

ASSUMPTION 2.3 (Coercivity). *There exist constants  $\gamma > 0$  and  $k_2 > 0$ , independent of  $k$ , such that (where  $\langle \cdot, \cdot \rangle_{L^2(\Gamma)}$  denotes the inner product in  $L^2(\Gamma)$ )*

$$\left| \langle \mathcal{A}\psi, \psi \rangle_{L^2(\Gamma)} \right| \geq \gamma \|\psi\|_{L^2(\Gamma)}^2, \quad \psi \in L^2(\Gamma), \quad k \geq k_2.$$

REMARK 2.4. *We note that, if Assumption 2.3 holds, then so does (2.6) for  $k_1 = k_2$  with  $C_1 = \gamma^{-1}$ . For the star-combined formulation with  $\mathcal{A} = \mathcal{A}_k$ , Assumption 2.3 holds with  $\gamma = (1/2) \operatorname{ess\,inf}_{\mathbf{x} \in \Gamma} (\mathbf{x} \cdot \mathbf{n}(\mathbf{x})) > 0$  for all  $k_2 > 0$  if  $\Omega$  is Lipschitz and star-like (in particular, if  $\Omega$  is a convex polygon) and  $\hat{\eta} = k|\mathbf{x}| + i/2$  as specified above (see [43] for details). By contrast, Assumption 2.3 has not been proved for the standard combined potential formulation except in the special case when the scatterer is circular (see [21]), although numerical evidence [7, Conjecture 6.2] suggests it holds more generally (in particular, for all convex polygons). We remark further that Assumption 2.3 is sufficient rather than necessary for our analysis; it is not necessary for Assumption 2.3 to hold for all  $k \geq k_2$ , but rather only for the specific wavenumber under consideration.*

**3. Analyticity and Regularity of Solutions.** Our goal is to derive a numerical method for the solution of the BIE (2.4) (and hence of the scattering problem), whose performance does not deteriorate significantly as the wavenumber  $k$  (which is proportional to frequency) increases, equivalently as the wavelength  $\lambda := 2\pi/k$  decreases. Specifically, we wish to avoid the requirement of conventional schemes for a fixed number of degrees of freedom per wavelength. To achieve this goal, our numerical method for solving (2.4) uses an approximation space (defined explicitly in §5) which is adapted to the high frequency asymptotic behaviour of the solution  $\partial u / \partial \mathbf{n}$  on each of the sides of the polygon, which we now consider. The results that follow in this section are for the case of a convex polygon.

We first define some notation. We label the corners of the polygon counterclockwise by  $\mathbf{P}_j$ ,  $j = 1, \dots, n_s$ , where  $n_s$  is the number of sides. In addition, we set  $\mathbf{P}_{n_s+1} := \mathbf{P}_1$ , and, for  $j = 1, \dots, n_s$ , denote the side between the corners  $\mathbf{P}_j$  and  $\mathbf{P}_{j+1}$  by  $\Gamma_j$ . We represent the point  $\mathbf{x} \in \Gamma$ , whose arc-length measured counterclockwise around  $\Gamma$  from  $\mathbf{P}_1$  is  $s$ , parametrically by

$$\mathbf{x}(s) = \mathbf{P}_j + \left(s - \tilde{L}_{j-1}\right) \left(\frac{\mathbf{P}_{j+1} - \mathbf{P}_j}{L_j}\right), \quad \text{for } s \in [\tilde{L}_{j-1}, \tilde{L}_j], \quad j = 1, \dots, n_s, \quad (3.1)$$

where  $L_j = |\mathbf{P}_{j+1} - \mathbf{P}_j|$  is the length of the side  $\Gamma_j$ , and  $\tilde{L}_j := \sum_{m=1}^j L_m$ ,  $j = 1, \dots, n_s$ , denotes the arc-length distance from  $\mathbf{P}_1$  to  $\mathbf{P}_{j+1}$ . We also set  $\tilde{L}_0 = 0$ , and denote the total length of  $\Gamma$  by  $L := \tilde{L}_{n_s}$ . We say that a side  $\Gamma_j$  is illuminated by the incident wave if  $\mathbf{d} \cdot \mathbf{n} < 0$  on  $\Gamma_j$ , and is in shadow if  $\mathbf{d} \cdot \mathbf{n} \geq 0$  on  $\Gamma_j$ . We denote by  $\Omega_j$  the exterior angle at the corner  $\mathbf{P}_j$ , and remark that for a convex polygon,  $\Omega_j \in (\pi, 2\pi)$  for all  $j = 1, \dots, n_s$ . Finally, let  $c_* > 0$  be a constant such that  $kL_j \geq c_*$  for all  $j = 1, \dots, n_s$  (e.g.  $c_* := \min_{j=1, \dots, n_s} \{kL_j\}$ ), and let  $L_* := \max_{j=1, \dots, n_s} \{L_j\}$ . These constants will play a key role in many of the estimates that follow.

Arguing as in [15, pp.621–623], on a typical side  $\Gamma_j$  we can write

$$\frac{\partial u}{\partial \mathbf{n}}(\mathbf{x}(s)) = \Psi(\mathbf{x}(s)) + v_j^+(s - \tilde{L}_{j-1})e^{iks} + v_j^-(\tilde{L}_j - s)e^{-iks}, \quad s \in [\tilde{L}_{j-1}, \tilde{L}_j],$$

$$j = 1, \dots, n_s, \quad (3.2)$$

where  $\Psi := 2\partial u^i / \partial \mathbf{n}$  if  $\Gamma_j$  is illuminated, and  $\Psi := 0$  if  $\Gamma_j$  is in shadow. Here, for  $j = 1, \dots, n_s$ ,

$$v_j^+(s) := \frac{ik^2}{2} \int_0^\infty e^{ik(t - \tilde{L}_{j-1})} \mu(k(s+t)) u(\mathbf{y}_j(\tilde{L}_{j-1} - t)) dt, \quad s \in [0, L_j], \quad (3.3)$$

$$v_j^-(s) := \frac{ik^2}{2} \int_0^\infty e^{ik(\tilde{L}_j + t)} \mu(k(s+t)) u(\mathbf{y}_j(\tilde{L}_j + t)) dt, \quad s \in [0, L_j], \quad (3.4)$$

where  $\mathbf{y}_j(s) := \mathbf{P}_j + (s - \tilde{L}_{j-1})(\mathbf{P}_{j+1} - \mathbf{P}_j)/L_j$  for  $s \in \mathbb{R}$ ,  $j = 1, \dots, n_s$ , and  $\mu(z) := e^{-iz} H_1^{(1)}(z)/z$  for  $z > 0$ . We remark that the decomposition (3.2) is very similar to [15, (3.9)], but here we have written the functions  $v_j^\pm(s)$  slightly differently, so that the singular nature of  $\partial u / \partial \mathbf{n}$  at the corners of the polygon manifests itself in singularities in  $v_j^\pm(s)$  at  $s = 0$  (see (3.5) below).

**REMARK 3.1.** *The representation (3.2) can be interpreted in terms of high frequency asymptotic theory as follows. The first term,  $\Psi$ , is the so-called ‘‘Physical Optics’’ approximation to  $\partial u / \partial \mathbf{n}$ , representing the direct contribution of the incident and reflected waves (where they are present). The second and third terms in (3.2) represent the contributions due to diffracted rays emanating from the corners  $\mathbf{P}_j$  and  $\mathbf{P}_{j+1}$ , respectively (see [15] for details).*

As will be described in more detail in §5, our numerical method uses an approximation space based on the representation (3.2), in which the factors  $v_j^\pm(s)$ ,  $s \in [0, L_j]$ ,  $j = 1, \dots, n_s$ , are approximated by piecewise polynomials, rather than approximating  $\partial u / \partial \mathbf{n}$  itself as in conventional methods. The advantage of our approach is that the functions  $v_j^\pm(s)$  are non-oscillatory, and can therefore be approximated much more efficiently than  $\partial u / \partial \mathbf{n}$ . Specifically, we have the following regularity assertion, which is the main result of the present section:



**THEOREM 3.2.** *The functions  $v_j^\pm(s)$ ,  $j = 1, \dots, n_s$ , are analytic in the right half-plane  $\operatorname{Re}[s] > 0$ , where they satisfy the bounds*

$$|v_j^\pm(s)| \leq \begin{cases} C_j^\pm M k |ks|^{-\delta_j^\pm}, & 0 < |s| \leq 1/k, \\ C_j^\pm M k |ks|^{-1/2}, & |s| > 1/k, \end{cases} \quad (3.5)$$

where  $\delta_j^+$ ,  $\delta_j^- \in (0, 1/2)$  are given by  $\delta_j^+ := 1 - \pi/\Omega_j$  and  $\delta_j^- := 1 - \pi/\Omega_{j+1}$  and  $M$  by

$$M := \sup_{\mathbf{x} \in D} |u(\mathbf{x})|. \quad (3.6)$$

For  $j = 1, \dots, n_s$ , the constants  $C_j^+$  depend only on  $c_*$  and  $\Omega_j$ , and the constants  $C_j^-$  depend only on  $c_*$  and  $\Omega_{j+1}$ .

**REMARK 3.3.** *The dependence of the constant  $M$  on the wavenumber  $k$  is not yet fully understood. In §4 we prove that, when  $\Omega$  is a star-like polygon,  $M = \mathcal{O}(k^{1/2} \log^{1/2} k)$  as  $k \rightarrow \infty$ . However, it is plausible, and supported by numerical experiments, that in fact  $M = \mathcal{O}(1)$  as  $k \rightarrow \infty$  in this case (and indeed for a more general class of polygons, see [13] for details).*

Bounds on the derivatives of the functions  $v_j^\pm(s)$  for  $s \in (0, \infty)$  have previously been derived in [15, Theorem 3.2, Corollary 3.4]. Here we show that it is possible to understand not just the behaviour of  $v_j^\pm(s)$  for  $s > 0$  but also to understand the behaviour of the analytic continuation of  $v_j^\pm(s)$  into the complex plane. This will be an essential component of our *hp* analysis, which follows in §5, but may also be of wider interest, as indicated in the Introduction. The proof of Theorem 3.2 relies on a number of intermediate results. We first note the following:

**LEMMA 3.4.** *The function  $\mu(z)$  is analytic in the half-plane  $\operatorname{Re}[z] > 0$ , with*

$$|\mu(z)| \leq \frac{2}{\pi} |z|^{-3/2} \left( |z|^{-1/2} + \sqrt{\frac{\pi}{2}} \right), \quad \operatorname{Re}[z] > 0. \quad (3.7)$$

*Proof.* By standard properties of the Hankel function  $H_1^{(1)}(z)$  (see e.g. [1, (10.7.2), (10.7.8)]),  $\mu(z)$  is analytic in the cut  $z$ -plane, with branch cut along the negative real axis. By [38, equation (12.32)],

$$\mu(z) = \frac{-2i}{\pi} \int_0^\infty (t^2 - 2it)^{1/2} e^{-zt} dt, \quad \operatorname{Re}[z] > 0, \quad (3.8)$$

where the branch of  $(t^2 - 2it)^{1/2}$  is chosen so that  $\operatorname{Re}[(t^2 - 2it)^{1/2}] \geq 0$  for  $t > 0$ . The integral in (3.8) is a parametrization of the contour integral

$$I(z) := \int_{\gamma_0} (w^2 - 2iw)^{1/2} e^{-zw} dw,$$

where  $\gamma_0$  runs along the positive real  $w$ -axis. Given  $z = re^{i\theta}$  with  $r > 0$  and  $\theta \in (-\pi/2, \pi/2)$  (so that  $\operatorname{Re}[z] > 0$ ), we may deform the contour of integration from  $\gamma_0$  onto the contour  $\gamma_\theta$  illustrated in Figure 3.1 (this is justified by the fact that for  $w = Re^{i\phi}$ , with  $\phi \in (-\theta, 0]$  for  $0 \leq \theta < \pi/2$  and  $\phi \in (0, -\theta)$  for  $-\pi/2 < \theta < 0$ , we have  $|e^{-zw}| \leq e^{-rR \cos \theta}$ , so that  $|e^{-zw}|$  tends to zero exponentially fast as  $R \rightarrow \infty$ , uniformly in  $\phi$ ). Parametrization of the integral over  $\gamma_\theta$ , with  $w = Re^{-i\theta}$ ,  $R > 0$ , then gives

$$I(z) = \int_{\gamma_\theta} (w^2 - 2iw)^{1/2} e^{-zw} dw = e^{-i\theta} \int_0^\infty (R^2 e^{-2i\theta} - 2iR e^{-i\theta})^{1/2} e^{-rR} dR,$$

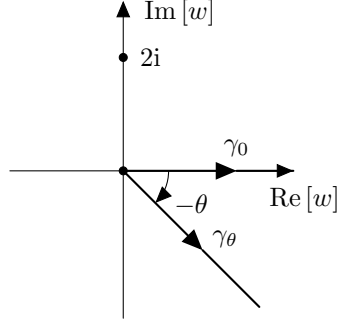


FIG. 3.1. The contours  $\gamma_0$  and  $\gamma_\theta$ .

so that

$$|I(z)| \leq \int_0^\infty R e^{-rR} dR + \sqrt{2} \int_0^\infty R^{1/2} e^{-rR} dR = \frac{1}{r^2} + \frac{\sqrt{\pi}}{\sqrt{2}r^{3/2}},$$

and the result follows.  $\square$

We now consider the solution behaviour near the corners.

LEMMA 3.5. *Suppose that  $\mathbf{x} \in D$  satisfies  $|\mathbf{x} - \mathbf{P}_j| =: r \in (0, 1/k]$ . Then there exists a constant  $C > 0$ , depending only on  $\Omega_j$  and  $c_*$ , such that (with  $M$  given by (3.6))*

$$|u(\mathbf{x})| \leq CM(kr)^{\pi/\Omega_j}.$$

*Proof.* Let  $(r, \theta)$  be polar coordinates local to a corner  $\mathbf{P}_j$ , chosen so that the side  $\Gamma_{j-1}$  lies on the line  $\theta = 0$  and the side  $\Gamma_j$  lies on the line  $\theta = \Omega_j$ . For  $R > 0$  let  $G_R \subset \bar{D}$  denote the set of points with polar coordinates  $\{(r, \theta) : 0 < r < R, 0 \leq \theta \leq \Omega_j\}$ . With  $R_j := \min\{L_{j-1}, L_j, \pi/(2k)\}$ , it follows from [15, Theorem 2.3] and [15, (3.14)] that, for  $0 < R < R_j$ ,

$$|u(\mathbf{x})| \leq \frac{2M(r/R)^{\pi/\Omega_j}}{\cos kR(1 - (r/R)^{\pi/\Omega_j})}, \quad \mathbf{x} \in G_R. \quad (3.9)$$

Now choose  $R = 3R_j/4$ , and suppose that  $0 < r < R_j/2$ . Then, since  $\min\{c_*, \pi/2\} \leq kR_j \leq \pi/2$ , (3.9) implies that

$$|u(\mathbf{x})| \leq \frac{2M(3 \min\{c_*, \pi/2\}/4)^{-\pi/\Omega_j}}{\cos(3\pi/8)(1 - (2/3)^{\pi/\Omega_j})} (kr)^{\pi/\Omega_j}, \quad \mathbf{x} \in G_{R_j/2}.$$

For  $R_j/2 \leq r \leq 1/k$  we may estimate

$$|u(\mathbf{x})| \leq M \leq \left(\frac{kR_j}{2}\right)^{-\pi/\Omega_j} M(kr)^{\pi/\Omega_j} \leq \left(\frac{\min\{c_*, \pi/2\}}{2}\right)^{-\pi/\Omega_j} M(kr)^{\pi/\Omega_j},$$

and the result follows.  $\square$

We are now ready to prove the main result of this section, Theorem 3.2.

*Proof.* (Proof of Theorem 3.2.) The analyticity of  $v_j^\pm(s)$  in  $\text{Re}[s] > 0$  is clear from (3.3)–(3.4) and Lemma 3.4. To prove the bounds (3.5) for  $v_j^+$  (the proof for  $v_j^-$  goes analogously and will be omitted here), we first note that

$$|v_j^+(s)| \leq \frac{k^2}{2} \int_0^\infty |\mu(k(s+t))| |u(\mathbf{y}_j(\tilde{L}_{j-1}-t))| dt. \quad (3.10)$$

If  $0 < |s| \leq 1/k$  then we split the integral in (3.10) into a sum of two integrals, the first over  $t \in (0, 1/k)$  and the second over  $t \in (1/k, \infty)$ . For the second integral, Lemma 3.4 implies that, since  $\text{Re}[s] > 0$ ,

$$\begin{aligned} \int_{1/k}^\infty |\mu(k(s+t))| |u(\mathbf{y}_j(\tilde{L}_{j-1}-t))| dt &\leq CM \int_{1/k}^\infty |k(s+t)|^{-3/2} dt \\ &\leq CM \int_{1/k}^\infty (kt)^{-3/2} dt = CMk^{-1}. \end{aligned}$$

For the first integral, we note from (3.7) that for  $|z| \leq 2$ ,  $\text{Re}[z] > 0$ , it follows that  $|\mu(z)| \leq C|z|^{-2}$ , and combining this with Lemma 3.5 we have

$$\begin{aligned} \int_0^{1/k} |\mu(k(s+t))| |u(\mathbf{y}_j(\tilde{L}_{j-1}-t))| dt &\leq CM \int_0^{1/k} |k(s+t)|^{-2} (kt)^{\pi/\Omega_j} dt \\ &\leq CM \int_0^{1/k} (k(|s|+t))^{-2} (kt)^{\pi/\Omega_j} dt \\ &= CMk^{-1} |ks|^{-\delta_j^+} \int_0^{1/(k|s|)} \frac{t^{\pi/\Omega_j}}{(t+1)^2} dt \\ &\leq CMk^{-1} |ks|^{-\delta_j^+}, \end{aligned}$$

where we recall that  $\delta_j^+ = 1 - \pi/\Omega_j$  and we have used the estimates

$$|s+t| \geq \frac{|s|+t}{\sqrt{2}}, \quad \text{Re}[s] > 0, \quad t \geq 0, \quad (3.11)$$

and

$$\int_0^{1/(k|s|)} \frac{t^{\pi/\Omega_j}}{(t+1)^2} dt \leq \int_0^\infty \frac{t^{\pi/\Omega_j}}{(t+1)^2} dt = \frac{\pi^2}{\Omega_j \sin(\pi(1-\pi/\Omega_j))}.$$

The integral over  $t \in (0, 1/k)$  therefore dominates the integral over  $t \in (1/k, \infty)$ , so that  $|v_j^+(s)| \leq CMk|ks|^{-\delta_j^+}$ , as claimed.

If  $|s| > 1/k$  then we do not need to split the integral in (3.10). Instead we simply use Lemma 3.4 and (3.11) to estimate

$$|v_j^+(s)| \leq CMk^2 \int_0^\infty |k(s+t)|^{-3/2} dt \leq CMk^2 \int_0^\infty (k(|s|+t))^{-3/2} dt = CMk|ks|^{-1/2},$$

as claimed.  $\square$

**4. Bounding  $M := \sup_{\mathbf{x} \in D} |u(\mathbf{x})|$ .** In this section we investigate the dependence of  $M := \sup_{\mathbf{x} \in D} |u(\mathbf{x})|$  on the wavenumber  $k$ . The main result of the section is Theorem 4.3, which gives a bound on  $M$  for the case where  $\Omega$  is a star-like polygon

(convex or non-convex). This result appears to be new, and could be used to improve the estimates of [15] directly, as well as being crucial to the  $k$ -explicit error analysis of our  $hp$  scheme which follows in §6. We begin with the following estimate of the norm of the single-layer potential operator in the domain.

LEMMA 4.1. *Let  $\Gamma$  be the boundary of an arbitrary polygon  $\Omega$  and let  $S_k : L^2(\Gamma) \rightarrow BC(\mathbb{R}^2)$  denote the single-layer potential in the domain,*

$$S_k \psi(\mathbf{x}) := \int_{\Gamma} \Phi_k(\mathbf{x}, \mathbf{y}) \psi(\mathbf{y}) \, ds(\mathbf{y}), \quad \mathbf{x} \in \mathbb{R}^2, \quad \psi \in L^2(\Gamma). \quad (4.1)$$

Then

$$\|S_k\|_{L^2(\Gamma) \rightarrow BC(\mathbb{R}^2)} \leq C_2 k^{-1/2} n_s^{1/2} \log^{1/2}(2 + kL_*), \quad k > 0,$$

where  $C_2 := \sqrt{5/(8 \log 2)}(1 + (2/\pi)(1 - \gamma_E + e^{1/4})) \approx 2.65$ , with  $\gamma_E \approx 0.577$  the Euler constant.

*Proof.* By the Cauchy-Schwarz inequality,

$$|S_k \psi(\mathbf{x})| \leq \|\Phi_k(\mathbf{x}, \cdot)\|_{L^2(\Gamma)} \|\psi\|_{L^2(\Gamma)}, \quad \mathbf{x} \in \mathbb{R}^2, \quad \psi \in L^2(\Gamma). \quad (4.2)$$

To estimate

$$\|\Phi_k(\mathbf{x}, \cdot)\|_{L^2(\Gamma)}^2 = \int_{\Gamma} |\Phi_k(\mathbf{x}, \mathbf{y})|^2 \, ds(\mathbf{y}) = \sum_{j=1}^{n_s} \int_{\Gamma_j} |\Phi_k(\mathbf{x}, \mathbf{y})|^2 \, ds(\mathbf{y}), \quad (4.3)$$

we note that, by the monotonic decay of  $|H_0^{(1)}(\cdot)|$  on  $(0, \infty)$  (see e.g. [46, §13.74]), each of the terms in the sum (4.3) can be individually maximised by taking  $\mathbf{x}$  to be the midpoint of  $\Gamma_j$ , so that

$$\|\Phi_k(\mathbf{x}, \cdot)\|_{L^2(\Gamma)}^2 \leq \frac{1}{8} \sum_{j=1}^{n_s} \int_0^{L_j/2} |H_0^{(1)}(kt)|^2 \, dt = \frac{1}{8k} \sum_{j=1}^{n_s} \int_0^{kL_j/2} |H_0^{(1)}(z)|^2 \, dz.$$

From [1, (10.2.2), (10.8.2) and (10.17.5)],

$$|H_0^{(1)}(z)| \leq \begin{cases} \hat{c}(1 + |\log z|), & 0 < z \leq 1, \\ \hat{c}z^{-1/2}, & z > 1, \end{cases}$$

where  $\hat{c} := 1 + (2/\pi)(1 - \gamma_E + e^{1/4}) \approx 2.09$ . Then for each  $j = 1, \dots, n_s$ , if  $kL_j/2 \leq 1$ ,

$$\int_0^{kL_j/2} |H_0^{(1)}(z)|^2 \, dz \leq \hat{c}^2 \int_0^1 (1 + |\log z|)^2 \, dz = 5\hat{c}^2,$$

and if  $kL_j/2 > 1$ ,

$$\int_0^{kL_j/2} |H_0^{(1)}(z)|^2 \, dz \leq \hat{c}^2 \left( \int_0^1 (1 + |\log z|)^2 \, dz + \int_1^{kL_j/2} z^{-1} \, dz \right) = \hat{c}^2 \left( 5 + \log \frac{kL_j}{2} \right).$$

These two possibilities are both covered by the estimate

$$\int_0^{kL_j/2} |H_0^{(1)}(z)|^2 \, dz \leq 5\hat{c}^2 \left( 1 + \max \left\{ 0, \log \frac{kL_j}{2} \right\} \right) \leq \frac{5\hat{c}^2}{\log 2} \log(2 + kL_j).$$

Hence

$$\|\Phi_k(\mathbf{x}, \cdot)\|_{L^2(\Gamma)}^2 \leq \frac{5\hat{c}^2}{8 \log 2} k^{-1} \sum_{j=1}^{n_s} \log(2 + kL_j) \leq \frac{5\hat{c}^2}{8 \log 2} k^{-1} n_s \log(2 + kL_*),$$

and, recalling (4.2), the result follows.  $\square$

Next, we require a bound on the norm of  $\partial u / \partial \mathbf{n}$ .

LEMMA 4.2. *For a star-like Lipschitz scatterer,*

$$\left\| \frac{\partial u}{\partial \mathbf{n}} \right\|_{L^2(\Gamma)} \leq \frac{L^{1/2} (1 + 4k \operatorname{diam} \Omega)}{\operatorname{ess\,inf}_{\mathbf{x} \in \Gamma} (\mathbf{x} \cdot \mathbf{n}(\mathbf{x}))}, \quad k > 0.$$

*Proof.* By (2.4),

$$\left\| \frac{\partial u}{\partial \mathbf{n}} \right\|_{L^2(\Gamma)} \leq \|\mathcal{A}^{-1}\|_{L^2(\Gamma)} \|f\|_{L^2(\Gamma)}, \quad (4.4)$$

and applying Lemma 2.2 with  $\mathcal{A} = \mathcal{A}_k$ , and recalling Remark 2.4, we have

$$\|\mathcal{A}^{-1}\|_{L^2(\Gamma)} \leq 2 / \operatorname{ess\,inf}_{\mathbf{x} \in \Gamma} (\mathbf{x} \cdot \mathbf{n}(\mathbf{x})), \quad k > 0. \quad (4.5)$$

It remains to bound  $\|f\|_{L^2(\Gamma)}$ , where  $f(\mathbf{x}) = \mathbf{x} \cdot \nabla u^i(\mathbf{x}) - i\hat{\eta}u^i(\mathbf{x})$  and  $\hat{\eta} = k|\mathbf{x}| + i/2$  (where  $\Omega$  is star-like with respect to the origin of our coordinate system). Recalling (2.1), we have  $\nabla u^i = ik\mathbf{d}u^i$ , and hence

$$|f(\mathbf{x})| = \left| k\mathbf{x} \cdot \mathbf{d} - k|\mathbf{x}| - \frac{i}{2} \right| \leq \frac{1}{2} + 2k|\mathbf{x}| \leq \frac{1}{2} + 2k \operatorname{diam} \Omega,$$

so that

$$\|f\|_{L^2(\Gamma)} \leq L^{1/2} \left( \frac{1}{2} + 2k \operatorname{diam} \Omega \right), \quad k > 0. \quad (4.6)$$

Inserting (4.5) and (4.6) into (4.4), the result follows.  $\square$

We are now ready to state and prove the main result of this section.

THEOREM 4.3. *For all  $k_3 > 0$ , if  $\Omega$  is a star-like polygon then*

$$M := \sup_{\mathbf{x} \in D} |u(\mathbf{x})| \leq C_3 k^{1/2} \log^{1/2}(2 + kL_*), \quad k \geq k_3,$$

where the constant  $C_3 > 0$  depends only on  $k_3$  and  $\Omega$ , specifically

$$C_3 = k_3^{-1/2} \log^{-1/2}(2 + k_3L_*) + \frac{C_2 n_s^{1/2} L^{1/2}}{\operatorname{ess\,inf}_{\mathbf{x} \in \Gamma} (\mathbf{x} \cdot \mathbf{n}(\mathbf{x}))} (k_3^{-1} + 4 \operatorname{diam} \Omega),$$

where  $C_2 \approx 2.65$  is the constant from Lemma 4.1.

*Proof.* Writing (2.3) as  $u(\mathbf{x}) = u^i(\mathbf{x}) - S_k \partial u / \partial \mathbf{n}(\mathbf{x})$ , for  $\mathbf{x} \in D$ , we estimate

$$M \leq 1 + \|S_k\|_{L^2(\Gamma) \rightarrow BC(\mathbb{R}^2)} \left\| \frac{\partial u}{\partial \mathbf{n}} \right\|_{L^2(\Gamma)},$$

so that by Lemmas 4.1 and 4.2,

$$M \leq 1 + \frac{C_2 n_s^{1/2} L^{1/2}}{\operatorname{ess\,inf}_{\mathbf{x} \in \Gamma} (\mathbf{x} \cdot \mathbf{n}(\mathbf{x}))} (k^{-1} + 4 \operatorname{diam} \Omega) k^{1/2} \log^{1/2}(2 + kL_*), \quad k > 0,$$

from which the result follows.  $\square$

**5.  $hp$  Approximation Space and Best Approximation Results.** We are now ready to design an approximation space  $V_{N,k} \subset L^2(\Gamma)$  to represent

$$\varphi(s) := \frac{1}{k} \left( \frac{\partial u}{\partial \mathbf{n}}(\mathbf{x}(s)) - \Psi(\mathbf{x}(s)) \right), \quad s \in [0, L], \quad (5.1)$$

based on (3.2). Here  $N$  denotes the total number of degrees of freedom in the method (to be elucidated later), and the subscript  $k$  on  $V_{N,k}$  serves to illustrate that our hybrid approximation space depends explicitly on the wavenumber  $k$ . The function  $\varphi$ , which we seek to approximate, can be thought of as the difference between  $\partial u / \partial \mathbf{n}$  and its ‘‘Physical Optics’’ approximation  $\Psi$  (recall Remark 3.1), scaled by  $1/k$  so that  $\varphi$  is nondimensional (cf. [15]). Instead of approximating  $\varphi$  directly by conventional piecewise polynomials, on each side  $\Gamma_j$ ,  $j = 1, \dots, n_s$ , we instead use the representation (3.2) with  $v_j^+(s - \tilde{L}_{j-1})$  and  $v_j^-(\tilde{L}_j - s)$ ,  $s \in [\tilde{L}_{j-1}, \tilde{L}_j]$ , replaced by piecewise polynomials supported on overlapping geometric meshes, graded towards the singularities at  $\mathbf{P}_j$  and  $\mathbf{P}_{j+1}$  respectively.

**DEFINITION 5.1.** *Given  $A > 0$  and an integer  $n > 0$  we denote by  $\mathcal{G}_n(0, A)$  the geometric mesh on  $[0, A]$  with  $n$  layers, whose meshpoints  $x_i$  are defined by*

$$x_0 := 0, \quad x_i := \sigma^{n-i} A, \quad i = 1, 2, \dots, n,$$

where  $0 < \sigma < 1$  is a grading parameter. Given a vector  $\mathbf{p} \in (\mathbb{N}_0)^n$  we denote by  $\mathcal{P}_{\mathbf{p},n}(0, A)$  the space of piecewise polynomials on the geometric mesh  $\mathcal{G}_n(0, A)$  with degree vector  $\mathbf{p}$ , i.e.

$$\mathcal{P}_{\mathbf{p},n}(0, A) := \left\{ \rho : [0, A] \rightarrow \mathbb{C} : \rho|_{(x_{i-1}, x_i)} \text{ is a polynomial of degree less than or equal to } (\mathbf{p})_i, i = 1, \dots, n \right\}.$$

In the case where  $(\mathbf{p})_i = p$  for all  $i = 1, \dots, n$ , for some integer  $p \geq 0$ , we write  $\mathcal{P}_{p,n}(0, A)$  for  $\mathcal{P}_{\mathbf{p},n}(0, A)$ .

A smaller value of  $\sigma$  represents a more severe grading. While the value  $\sigma = (\sqrt{2} - 1)^2 \approx 0.17$  is in some sense optimal, [42, p.96], [23], it is common practice to slightly ‘‘overrefine’’ by taking  $\sigma = 0.15$ ; in our numerical experiments of §7 we take  $\sigma = 0.15$ .

For each  $j = 1, \dots, n_s$  let integers  $N_j^\pm \geq 1$  and degree vectors  $\mathbf{p}_j^\pm \in (\mathbb{N}_0)^n$  be given. We then define the spaces

$$V_j^+ := \left\{ \rho(s) e^{iks} : \rho|_{(\tilde{L}_{j-1}, \tilde{L}_j)}(s) = \tilde{\rho}(s - \tilde{L}_{j-1}), \tilde{\rho} \in \mathcal{P}_{\mathbf{p}_j^+, N_j^+}(0, L_j), \rho|_{(0, \tilde{L}_{j-1}) \cup (\tilde{L}_j, L)} = 0 \right\},$$

$$V_j^- := \left\{ \rho(s) e^{-iks} : \rho|_{(\tilde{L}_{j-1}, \tilde{L}_j)}(s) = \tilde{\rho}(\tilde{L}_j - s), \tilde{\rho} \in \mathcal{P}_{\mathbf{p}_j^-, N_j^-}(0, L_j), \rho|_{(0, \tilde{L}_{j-1}) \cup (\tilde{L}_j, L)} = 0 \right\}.$$

As we shall show in Theorem 5.4,  $V_j^+$  and  $V_j^-$  are well-adapted to approximating respectively the terms  $v_j^+(s - \tilde{L}_{j-1})e^{iks}$  and  $v_j^-(\tilde{L}_j - s)e^{-iks}$  in the representation (3.2). Our approximation space  $V_{N,k}$  is then defined explicitly by

$$V_{N,k} := \text{span} \left\{ \bigcup_{j=1}^{n_s} (V_j^+ \cup V_j^-) \right\}, \quad (5.2)$$

and the total number of degrees of freedom is

$$N := \dim(V_{N,k}) = \sum_{j=1}^{n_s} \left( \sum_{m=1}^{N_j^+} ((\mathbf{p}_j^+)_m + 1) + \sum_{m=1}^{N_j^-} ((\mathbf{p}_j^-)_m + 1) \right). \quad (5.3)$$

The regularity results provided by Theorem 3.2 allow us to prove that, under appropriate assumptions on the choices of  $N_j^\pm$  and  $\mathbf{p}_j^\pm$ , the best approximation error in approximating  $\varphi$  by an element of  $V_{N,k}$  decays exponentially as the maximum degree of the approximating polynomials increases.

For simplicity of presentation we shall assume henceforth that the degree of polynomial approximation is constant within each mesh, so that

$$(\mathbf{p}_j^\pm)_m = p_j^\pm, \quad m = 1, \dots, N_j^\pm, \quad (5.4)$$

for some integers  $p_j^\pm \geq 0$ ,  $j = 1, \dots, n_s$ , and (5.3) becomes

$$N = \sum_{j=1}^{n_s} (N_j^+ (p_j^+ + 1) + N_j^- (p_j^- + 1)). \quad (5.5)$$

However, we note that variations offering the same asymptotic convergence rates with a reduced total number of degrees of freedom are also possible; in particular see Remark 5.3 below. The following theorem shows that piecewise polynomial approximation on a geometric mesh leads to exponential convergence. While we refer the reader to Appendix A for the details, we point the reader to the arguments preceding [5, Thm. 2.5], where a similar exponential convergence result is shown without the aim of sharp estimates for the constants involved. We also refer to [23, 24, 42, 34, 41] for related results.

**THEOREM 5.2.** *Suppose that a function  $g(z)$  is analytic in  $\operatorname{Re}[z] > 0$  and satisfies, for some  $\hat{C} > 0$  and  $0 \leq \delta < 1/2$ , the bounds*

$$|g(z)| \leq \begin{cases} \hat{C}|z|^{-\delta}, & 0 < |z| \leq 1, \\ \hat{C}|z|^{-1/2}, & |z| > 1. \end{cases} \quad (5.6)$$

Then, for  $A > 0$ , and for integers  $n \geq 1$  and  $p \geq 0$ ,

(i) *there exists a constant  $C > 0$ , depending only on  $\delta$  and  $\sigma$ , such that the best  $L^2$  approximation error in  $\mathcal{P}_{p,n}(0, A)$  satisfies*

$$\inf_{v \in \mathcal{P}_{p,n}(0, A)} \|g - v\|_{L^2(0, A)} \leq C \hat{C} \left( A^{1/2-\delta} e^{-n\vartheta} + \log^{1/2}(2 + A) e^{-p\xi} \right), \quad (5.7)$$

where  $\vartheta = |\log \sigma| (1/2 - \delta)$  and

$$\xi = \log \left( \frac{1 + \sigma^{1/2}(2 - \sigma)^{1/2}}{1 - \sigma} \right) > 0; \quad (5.8)$$

(ii) *furthermore, if  $n$  is chosen such that  $n \geq cp$  for some constant  $c > 0$ , then*

$$\inf_{v \in \mathcal{P}_{p,n}(0, A)} \|g - v\|_{L^2(0, A)} \leq C \hat{C} \left( A^{1/2-\delta} + \log^{1/2}(2 + A) \right) e^{-p\tau}, \quad (5.9)$$

where  $\tau = \min \{c\vartheta, \xi\} > 0$ .

**REMARK 5.3.** *It is possible to reduce the total number of degrees of freedom, whilst maintaining exponential convergence as the maximum polynomial degree tends to infinity, by relaxing the assumption (5.4) and using a lower degree approximation near the singularity. For example, given  $p \geq 1$ , suppose that we define a degree vector  $\mathbf{p}$  by*

$$(\mathbf{p})_i := \begin{cases} \left\lfloor \frac{i-1}{n_*} p \right\rfloor, & 1 \leq i \leq n_*, \\ p, & n_* + 1 \leq i \leq n, \end{cases}$$

where  $n_*$  is the largest  $i \in \{1, \dots, n\}$  such that  $\frac{x_{i-1}}{2} < 1$ . Then one can prove best approximation estimates similar to (5.7) and (5.9) in the space  $\mathcal{P}_{\mathbf{p},n}(0, A)$ . For further details see Appendix A, Theorem A.3.

Combining Theorem 5.2 with Theorem 3.2 we can then deduce the following best approximation result:

**THEOREM 5.4.** *Suppose that*

$$N_j^\pm \geq c_j^\pm p_j^\pm, \quad (5.10)$$

for some  $c_j^\pm > 0$ . Then there exist constants  $\hat{C}_j^+ > 0$ , depending only on  $\sigma$ ,  $c_*$  and  $\Omega_j$ , and  $\hat{C}_j^- > 0$ , depending only on  $\sigma$ ,  $c_*$  and  $\Omega_{j+1}$ , such that

$$\inf_{v \in \mathcal{P}_{p_j^\pm, N_j^\pm}(0, L_j)} \|v_j^\pm - v\|_{L^2(0, L_j)} \leq \hat{C}_j^\pm M k^{1/2} \left( (kL_j)^{1/2 - \delta_j^\pm} + \log^{1/2}(2 + kL_j) \right) e^{-p_j^\pm \tau_j^\pm},$$

where  $\tau_j^\pm = \min \{c_j^\pm |\log \sigma| (1/2 - \delta_j^\pm), \xi\} > 0$ .

*Proof.* Applying Theorem 5.2 to  $g(z) := v_j^\pm(z/k)$ , which, by Theorem 3.2, satisfies the bounds (5.6) with  $\hat{C} = C_j^\pm M k$  and  $\delta = \delta_j^\pm$ , and noting that

$$\inf_{v \in \mathcal{P}_{p_j^\pm, N_j^\pm}(0, L_j)} \|v_j^\pm - v\|_{L^2(0, L_j)} = \frac{1}{k^{1/2}} \inf_{w \in \mathcal{P}_{p_j^\pm, N_j^\pm}(0, kL_j)} \|g - w\|_{L^2(0, kL_j)},$$

the result follows.  $\square$

We conclude this section with an estimate for the best approximation error associated with the approximation of  $\varphi$  on  $\Gamma$  by an element of  $V_{N,k}$ . We assume here that (5.4) holds, but a similar result holds when the polynomial degree is reduced towards the singularities, as outlined in Remark 5.3 above. Here and in what follows we make the obvious identification between  $L^2(\Gamma)$  and  $L^2(0, L)$ , via the parametrization  $\mathbf{x}(s)$ .

**THEOREM 5.5.** *Suppose that (5.10) holds for each  $j = 1, \dots, n_s$ . Then, with  $p := \max_{j,\pm} \{p_j^\pm\}$ , there exists a constant  $C_4 > 0$ , depending only on  $\{\Omega_j\}_{j=1}^{n_s}$ ,  $\sigma$  and  $c_*$ , and a constant  $\tau > 0$ , depending only on  $\{\Omega_j\}_{j=1}^{n_s}$ ,  $\sigma$ , and  $\{c_j^\pm\}_{j=1}^{n_s}$ , such that*

$$\inf_{v \in V_{N,k}} \|\varphi - v\|_{L^2(\Gamma)} \leq C_4 M k^{-1/2} G(k) e^{-p\tau}, \quad (5.11)$$

where

$$G(k) := (1 + kL_*)^{1/2 - \delta_*} + \log^{1/2}(2 + kL_*),$$

and  $\delta_* := \min_{j,\pm} \{\delta_j^\pm\}$ .

*Proof.* Recalling (3.2) and (5.1), the result follows straight from Theorem 5.4, with e.g.  $C_4 = \sum_{j=1}^{n_s} (\hat{C}_j^+ + \hat{C}_j^-)$  and  $\tau = \min_{j,\pm} \{p_j^\pm \tau_j^\pm\} / p$ .  $\square$

**REMARK 5.6.** *We note that the constants  $C_4$  and  $\tau$  in Theorem 5.5 depend on the corner angles  $\{\Omega_j\}_{j=1}^{n_s}$  of the polygon. In particular, we expect that  $C_4 \rightarrow \infty$  and  $\tau \rightarrow 0$  as  $\Omega_j \rightarrow 2\pi$  (i.e. as  $\delta_j^+, \delta_{j-1}^- \rightarrow 1/2$ ) for one or more  $j$ . This is because when  $\delta \rightarrow 1/2$  in Theorem 5.2, the constant  $C$  in (5.7) and (5.9) blows up like  $1/(1/2 - \delta)$  (for details, see the proof of Theorem 5.2 in Appendix A), and the constant  $\vartheta$  tends to zero like  $1/2 - \delta$ . Such behaviour is of course to be expected, since when  $\delta = 1/2$  in (5.6) we no longer expect  $g \in L^2(0, A)$ . This issue has implications for the accuracy, measured in the  $L^2$  norm, of the solution of our Galerkin BEM (described in the next section). Importantly, however, and as we demonstrate in §7 via numerical examples, this issue does not seem to affect the accuracy of the solution in the domain, the far field pattern, or indeed the boundary solution when measured in the weaker  $L^1$  norm.*



**6. Galerkin Method.** Having designed an approximation space  $V_{N,k}$  which can efficiently approximate  $\varphi$ , we now select an element of  $V_{N,k}$  using the Galerkin method. That is, we seek  $\varphi_N \in V_{N,k} \subset L^2(\Gamma)$  such that (recall (2.4) and (5.1))

$$\langle \mathcal{A}\varphi_N, v \rangle_{L^2(\Gamma)} = \frac{1}{k} \langle f - \mathcal{A}\Psi, v \rangle_{L^2(\Gamma)}, \quad \text{for all } v \in V_{N,k}. \quad (6.1)$$

The existence and uniqueness of the Galerkin solution  $\varphi_N$  is guaranteed by the coercivity assumption, Assumption 2.3 (see e.g. [27, Theorem 13.27]). Moreover, Lemma 2.1, Assumption 2.3 and Céa's lemma together imply the quasi-optimality estimate

$$\|\varphi - \varphi_N\|_{L^2(\Gamma)} \leq \frac{C_0 k^{1/2}}{\gamma} \inf_{v \in V_{N,k}} \|\varphi - v\|_{L^2(\Gamma)}, \quad k \geq k_2,$$

where  $C_0$  is the constant from Lemma 2.1 (under the choice  $k_0 = k_2$ ), and  $\gamma$  and  $k_2$  are the constants from Assumption 2.3. Combined with Theorem 5.5, this gives:

**THEOREM 6.1.** *If Assumption 2.3 and the assumptions of Theorem 5.5 hold, then*

$$\|\varphi - \varphi_N\|_{L^2(\Gamma)} \leq \frac{C_0 C_4 M}{\gamma} G(k) e^{-p\tau}, \quad k \geq k_2, \quad (6.2)$$

where  $C_0$ ,  $\gamma$  and  $k_2$  are as above, and  $C_4$ ,  $\tau$  and  $G(k)$  are as in Theorem 5.5.

Combining Theorem 6.1 with the bound on  $M$  established in Theorem 4.3, we obtain an error estimate which is completely explicit in its  $k$ -dependence:

**COROLLARY 6.2.** *Under the assumptions of Theorem 6.1 we have*

$$\|\varphi - \varphi_N\|_{L^2(\Gamma)} \leq C_5 k^{1/2} \log^{1/2}(2 + kL_*) G(k) e^{-p\tau}, \quad k \geq k_2, \quad (6.3)$$

where  $C_5 := C_0 C_3 C_4 / \gamma$  and  $C_3$  is the constant from Theorem 4.3 (with  $k_3 = k_2$ ).

An approximation  $u_N$  to the solution  $u$  of the BVP can be found by inserting the approximation  $(\partial u / \partial \mathbf{n})(\mathbf{x}(s)) \approx \Psi(\mathbf{x}(s)) + k\varphi_N(s)$  into the formula (2.3), i.e.

$$u_N(\mathbf{x}) := u^i(\mathbf{x}) - \int_0^L \Phi_k(\mathbf{x}, \mathbf{y}(s)) (\Psi(\mathbf{y}(s)) + k\varphi_N(s)) ds, \quad \mathbf{x} \in D,$$

where  $\mathbf{y}(s)$  is defined exactly as  $\mathbf{x}(s)$  was in (3.1). We then have the following error estimate, which again is completely explicit in its  $k$ -dependence:

**THEOREM 6.3.** *Under the assumptions of Theorem 6.1 we have*

$$\frac{\|u - u_N\|_{L^\infty(D)}}{\|u\|_{L^\infty(D)}} \leq C_6 k^{1/2} \log^{1/2}(2 + kL_*) G(k) e^{-p\tau}, \quad k \geq k_2, \quad (6.4)$$

where  $C_6 = C_0 C_2 C_4 n_s^{1/2} / \gamma$  and  $C_2$  is the constant from Lemma 4.1.

*Proof.* For  $\mathbf{x} \in D$ ,

$$|u(\mathbf{x}) - u_N(\mathbf{x})| = k |S_k(\varphi - \varphi_N)(\mathbf{x})| \leq k \|S_k\|_{L^2(\Gamma) \rightarrow BC(\mathbb{R}^2)} \|\varphi - \varphi_N\|_{L^2(\Gamma)}, \quad (6.5)$$

with  $S_k$  given by (4.1), and the result follows from Lemma 4.1 and Theorem 6.1.  $\square$

An object of interest in applications is the *far field pattern* of the scattered field. An asymptotic expansion of the representation (2.3) reveals that (cf. [18])

$$u^s(\mathbf{x}) \sim \frac{e^{i\pi/4}}{2\sqrt{2\pi}} \frac{e^{ikr}}{\sqrt{kr}} F(\hat{\mathbf{x}}), \quad \text{as } r := |\mathbf{x}| \rightarrow \infty,$$

where the origin  $\mathbf{x} = 0$  is assumed to lie inside  $\Omega$ ,  $\hat{\mathbf{x}} := \mathbf{x}/|\mathbf{x}| \in \mathbb{S}^1$ , the unit circle, and

$$F(\hat{\mathbf{x}}) := - \int_{\Gamma} e^{-ik\hat{\mathbf{x}} \cdot \mathbf{y}} \frac{\partial u}{\partial \mathbf{n}}(\mathbf{y}) \, ds(\mathbf{y}), \quad \hat{\mathbf{x}} \in \mathbb{S}^1. \quad (6.6)$$

An approximation  $F_N$  to the far field pattern  $F$  can be found by inserting the approximation  $(\partial u / \partial \mathbf{n})(\mathbf{x}(s)) \approx \Psi(\mathbf{x}(s)) + k\varphi_N(s)$  into the formula (6.6), i.e.

$$F_N(\hat{\mathbf{x}}) := - \int_0^L e^{-ik\hat{\mathbf{x}} \cdot \mathbf{y}(s)} (\Psi(\mathbf{y}(s)) + k\varphi_N(s)) \, ds, \quad \hat{\mathbf{x}} \in \mathbb{S}^1. \quad (6.7)$$

**THEOREM 6.4.** *Under the assumptions of Theorem 6.1 we have*

$$\|F - F_N\|_{L^\infty(\mathbb{S}^1)} \leq C_5 L^{1/2} k^{3/2} \log^{1/2}(2 + kL_*) G(k) e^{-p\tau}, \quad k \geq k_2, \quad (6.8)$$

where  $C_5$  is the constant from Corollary 6.2.

*Proof.* By the Cauchy-Schwarz inequality,

$$|F(\hat{\mathbf{x}}) - F_N(\hat{\mathbf{x}})| \leq k \int_0^L |\varphi(s) - \varphi_N(s)| \, ds \leq kL^{1/2} \|\varphi - \varphi_N\|_{L^2(\Gamma)}, \quad \hat{\mathbf{x}} \in \mathbb{S}^1, \quad (6.9)$$

and the result follows from Corollary 6.2.  $\square$

**REMARK 6.5.** *The algebraically  $k$ -dependent prefactors in the error estimates (6.2), (6.3), (6.4) and (6.8) can be absorbed into the exponentially decaying factors by allowing  $p$  to grow modestly with increasing  $k$ . Let us illustrate this point in the case of (6.4). Clearly, (6.4) implies the weaker (but simpler) bound*

$$\frac{\|u - u_N\|_{L^\infty(D)}}{\|u\|_{L^\infty(D)}} \leq C_7 (2 + kL_*)^{3/2} e^{-p\tau}, \quad k \geq k_2, \quad (6.10)$$

where  $C_7 := 2C_6/L^{1/2}$ . If we assume, in addition to the assumptions of Theorem 6.1, that

$$p \geq \frac{3 \log(2 + kL_*)}{2c_2}, \quad (6.11)$$

for some  $0 < c_2 < \tau$ , then (6.10), and hence (6.4), can be replaced by

$$\frac{\|u - u_N\|_{L^\infty(D)}}{\|u\|_{L^\infty(D)}} \leq C_7 e^{-p\kappa}, \quad k \geq k_2, \quad (6.12)$$

where  $\kappa = \tau - c_2$ , and both  $\kappa$  and  $C_7$  are independent of  $k$ . Recalling (5.5), it follows from (5.10), (6.11) and (6.12) that in order to maintain a fixed accuracy of approximation, we need only increase the number of degrees of freedom like  $\mathcal{O}(\log^2 k)$  as  $k \rightarrow \infty$ .

**7. Numerical Results.** We now present numerical results for the solution of (6.1). We consider two different polygonal scatterers, an equilateral triangle and a regular pentagon. In each case the sides of the polygon are of length  $2\pi$ , so the number of wavelengths per side is equal to  $k$ . The scatterers, the incident direction vectors  $\mathbf{d}$  (recall (2.1)), the corresponding total fields for  $k = 10$ , and a circle of radius  $2\pi$  on which we compute the total field (see Figures 7.3 and 7.4 below), are plotted in Figure 7.1. For both scatterers we demonstrate exponential decay of the  $L_2$  norm of the error

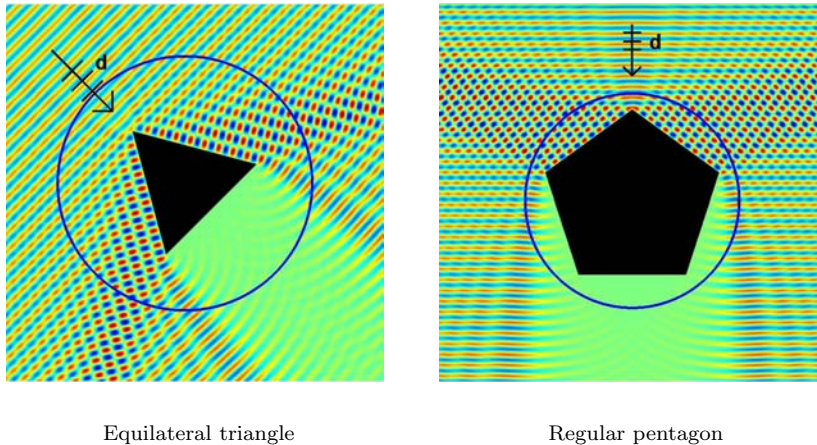


FIG. 7.1. Scattering configurations and plots of the real part of  $u = u^i + u^s$ , for  $k = 10$ .

on the boundary as  $p$  increases, with only very mild dependence on the wavenumber  $k$ , as predicted by (6.2) and (6.3). We also demonstrate how these results extend to the computation of both the solution in the domain and the far field pattern, error estimates for which are given in (6.4) and (6.8), and we investigate how the accuracy of our results depends on the geometry of the scatterer. The results presented here are computed using the standard combined potential formulation, with  $\mathcal{A} = \mathcal{A}_{k,\eta}$ ; we make this choice because we wish to demonstrate that our numerical results are entirely consistent with our theoretical predictions, even though we do not yet have a complete theory for this case (since, as discussed in Remark 2.4, Assumption 2.3 has not yet been shown to hold for  $\mathcal{A} = \mathcal{A}_{k,\eta}$ ). In all of our experiments we take the same degree  $p$  of polynomial approximation on each element, and the same number of layers  $N_l := 2(p+1)$  on each graded mesh. According to (5.5), with  $N_j^\pm = N_l$  and  $p_j^\pm = p$  for each  $j = 1, \dots, n_s$ , the total number of degrees of freedom is given by

$$N = 4n_s(p+1)^2. \quad (7.1)$$

Since for each example  $N$  depends only on  $p$  (through (7.1)), we simplify our presentation by defining  $\psi_p(s) := \varphi_N(s)$ . For the purposes of comparison with the theoretical results, we note that in both examples (5.10) is satisfied with  $c_j^\pm = 2$  for each  $j = 1, \dots, n_s$ .

In Figure 7.2 we plot the relative  $L^2$  and  $L^1$  errors (each on a logarithmic scale) against  $p$ , for both examples and for a range of values of  $k$ . In each case we take the “exact” reference solution to be that computed with  $p = 7$ ; further verification of our method via comparison with solutions computed using the  $h$ -version scheme of [15], with a large number of degrees of freedom, has also been performed, but is not reported in detail here. The  $L^2$  and  $L^1$  norms are computed by a high-order composite Gaussian quadrature scheme on a mesh graded towards the corner singularities; experimental evidence suggests that these calculations are accurate to at least four digits of precision (a far higher accuracy than that achieved by the corresponding quadrature scheme in [15], which used a uniform mesh).

The linear plots in Figure 7.2 clearly demonstrate exponential decay with increas-

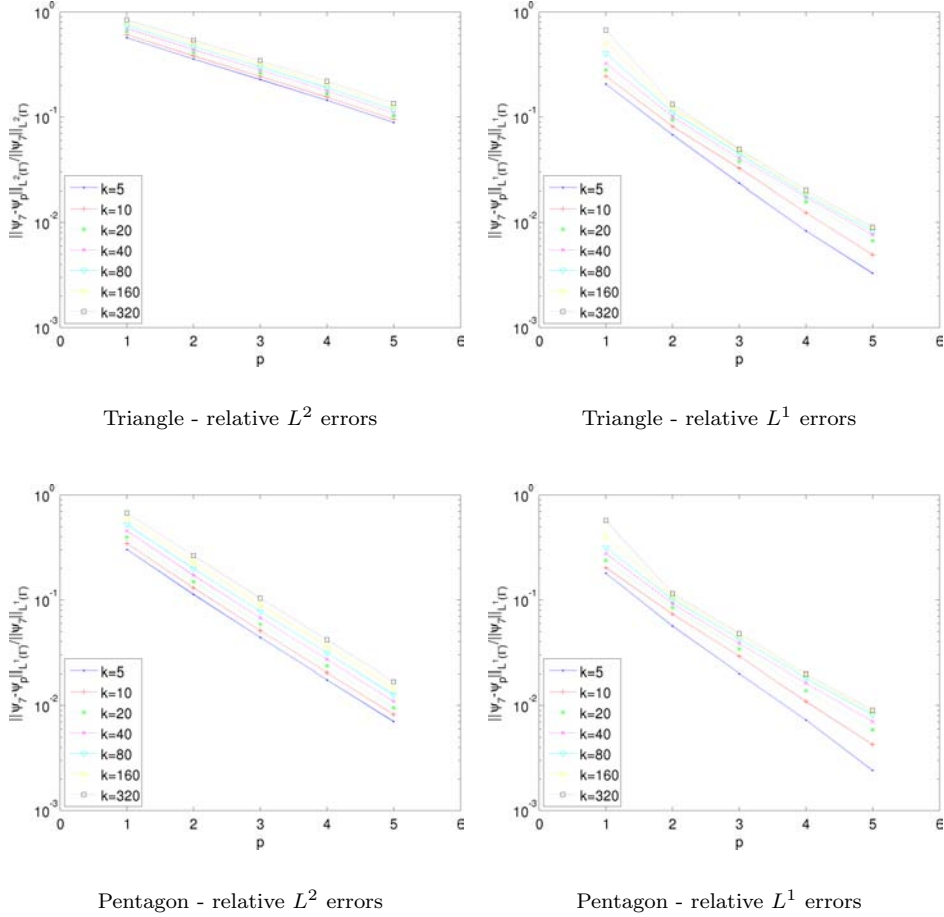


FIG. 7.2. Relative  $L^2$  and  $L^1$  errors in boundary solution.

ing polynomial degree  $p$ , as predicted for the  $L^2$  error by Theorem 6.2. We shall make comparisons between the four plots in Figure 7.2 shortly. However, we first focus on the key question of how the accuracy of our results depends on the parameter  $k$ .

In all four plots in Figure 7.2 the relative errors increase only very mildly as  $k$  increases. To investigate this further, in Table 7.1 we show results for the equilateral triangle for fixed  $p = 4$  (and hence fixed  $N = 300$ ), for a larger range of  $k$ . As well as showing absolute  $L^2$  errors and relative  $L^2$  and  $L^1$  errors, we also show  $N/(L/\lambda)$ , the average number of degrees of freedom per wavelength. For the same value of  $N$ , as  $k$  increases, the relative errors increase only mildly, and the absolute  $L^2$  error actually decreases, despite the average number of degrees of freedom per wavelength decreasing. It is interesting to compare these results to the  $k$ -explicit theoretical estimate (6.3) for the absolute  $L^2$  error in Corollary 6.2. Suppose we make the hypothesis that  $\text{error}(k) \sim k^\alpha$  as  $k \rightarrow \infty$ , where  $\text{error}(k)$  refers to the absolute  $L^2$  error for a particular value of  $k$ , and  $\alpha$  denotes the estimated order of growth ( $\alpha > 0$ ) or decay ( $\alpha < 0$ ). Under this hypothesis, we calculate  $\alpha := \log_2(\text{error}(2k)/\text{error}(k))$ , and if the hypothesis is correct we would anticipate  $\alpha$  to take approximately constant values for

$k$	$\frac{N}{L/\lambda}$	$\ \psi_7 - \psi_4\ _{L^2(\Gamma)}$	$\alpha$	$\frac{\ \psi_7 - \psi_4\ _{L^2(\Gamma)}}{\ \psi_7\ _{L^2(\Gamma)}}$	$\frac{\ \psi_7 - \psi_4\ _{L^1(\Gamma)}}{\ \psi_7\ _{L^1(\Gamma)}}$	COND	cpt(s)
5	20.00	$1.96 \times 10^{-1}$	-0.40	$1.44 \times 10^{-1}$	$8.33 \times 10^{-3}$	$3.50 \times 10^2$	621
10	10.00	$1.48 \times 10^{-1}$	-0.40	$1.55 \times 10^{-1}$	$1.24 \times 10^{-2}$	$2.77 \times 10^1$	612
20	5.00	$1.12 \times 10^{-1}$	-0.40	$1.66 \times 10^{-1}$	$1.58 \times 10^{-2}$	$3.51 \times 10^1$	600
40	2.50	$8.50 \times 10^{-2}$	-0.40	$1.78 \times 10^{-1}$	$1.74 \times 10^{-2}$	$4.60 \times 10^1$	691
80	1.25	$6.44 \times 10^{-2}$	-0.40	$1.91 \times 10^{-1}$	$1.83 \times 10^{-2}$	$6.12 \times 10^1$	665
160	0.63	$4.88 \times 10^{-2}$	-0.40	$2.04 \times 10^{-1}$	$1.91 \times 10^{-2}$	$8.27 \times 10^1$	648
320	0.31	$3.70 \times 10^{-2}$	-0.40	$2.19 \times 10^{-1}$	$2.02 \times 10^{-2}$	$1.12 \times 10^2$	746
640	0.16	$2.80 \times 10^{-2}$	-0.38	$2.35 \times 10^{-1}$	$2.06 \times 10^{-2}$	$1.53 \times 10^2$	746
1280	0.08	$2.16 \times 10^{-2}$	-0.39	$2.55 \times 10^{-1}$	$2.19 \times 10^{-2}$	$2.08 \times 10^2$	764
2560	0.04	$1.65 \times 10^{-2}$	-0.39	$2.76 \times 10^{-1}$	$2.19 \times 10^{-2}$	$2.83 \times 10^2$	826
5120	0.02	$1.26 \times 10^{-2}$		$2.97 \times 10^{-1}$	$2.25 \times 10^{-2}$	$3.85 \times 10^2$	823

TABLE 7.1

$L^2$  and  $L^1$  errors for the triangle, fixed  $p = 4$  (and hence  $N = 300$ ), various  $k$ .

$k$  sufficiently large. Recalling (6.3), we might expect to see  $\alpha \geq \max_{j=1, \dots, n_s} (1 - \delta_j^\pm)$ ; for the equilateral triangle  $\delta_j^\pm = 1 - \pi/(5\pi/3)$ , for  $j = 1, 2, 3$ , suggesting an anticipated value  $\alpha \geq 3/5$ . But the results in Table 7.1 show  $\alpha \approx -2/5$ . This suggests that our estimate (6.3) is not sharp in terms of its  $k$ -dependence. It is interesting to note that the observed value  $\alpha \approx -2/5$  is actually consistent with the  $k$ -dependence of our *best approximation* estimate (5.11), if we assume that  $M = \mathcal{O}(1)$  as  $k \rightarrow \infty$  (cf. Remark 3.3).

We also show in Table 7.1 the 2-norm condition number (COND) of the linear system arising from the discretization of (6.1). The condition number grows only slowly as  $k$  increases for fixed  $p$ . This is in contrast to methods where the approximation space consists of standard finite element basis functions multiplied by plane waves travelling in many directions, for which large condition numbers can cause significant difficulties; see e.g. [31] and the references therein. In the final column of Table 7.1, we also show the computing time (cpt), measured in seconds, required to construct and solve the linear system in each case. The computing time increases only slowly (if at all) as the wavenumber  $k$  increases. For details of how this is achieved, see [35]. These results were computed using Matlab on a Dell T7400 2.83GHz machine. We expect that faster computation times could be achieved with some optimization of the code.

We now return to compare the four plots in Figure 7.2. As already alluded to in Remark 5.6, our  $L^2$  best approximation estimates in §5 are not uniform with respect to variations in the corner angles of the polygon; this is linked to the fact that the  $L^2$  norm of the boundary solution blows up if  $\Omega_j \rightarrow 2\pi$  for any  $j = 1, \dots, n_s$  (i.e. as the corners become sharper). Figure 7.2 suggest that this nonuniformity also appears in our numerical solutions, since, comparing the  $L^2$  errors for the triangle and the pentagon, we see that, although in each case the error is decaying exponentially with increasing polynomial degree, the errors are significantly greater in magnitude (with slower rate of decay) for the triangle than they are for the pentagon (note that each of the four plots in Figure 7.2 is on the same scale).

On the other hand, Lemma 3.5 implies that for  $q < 2$  the weaker  $L^q$  norm of the solution on the boundary remains bounded, even as  $\Omega_j \rightarrow 2\pi$ . The plots in Figure 7.2 reflect this, with the errors in the  $L^1$  norm being much smaller than the

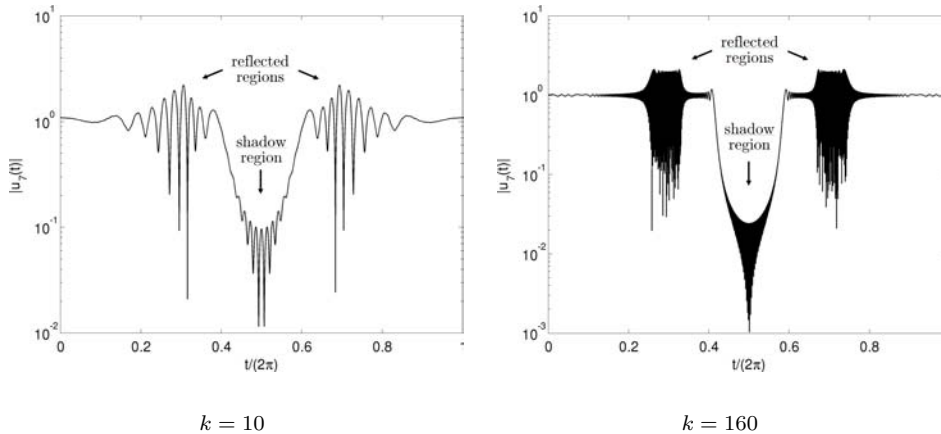


FIG. 7.3. Total field for the triangle, evaluated on the circle of Figure 7.1.

corresponding  $L^2$  errors, and this difference being particularly pronounced for the scatterer with sharper corners (the triangle). Moreover, there is little difference in either the magnitude or rate of decay of the  $L^1$  errors between the two examples, which suggests that the  $L^1$  error is not significantly affected by corner angles. We return to this observation at the end of the paper.

We now turn our attention to the approximation of  $u(\mathbf{x})$ ,  $\mathbf{x} \in D$ , and of the far field pattern  $F$  (often the quantities of real interest in scattering problems). As might be expected of linear functionals of the boundary solution, we find that the errors in  $u(\mathbf{x})$  and  $F$  are, in general, much smaller than the relative errors in  $\varphi$ . Moreover, the sensitivity to the corner angles seen in the  $L^2$  errors in  $\varphi$  does not seem to be present in the approximations of  $u(\mathbf{x})$  and  $F$ .

To investigate the accuracy of our solution in the domain, we compute the solution on a circle of radius  $2\pi$  surrounding the scatterer, as illustrated in Figure 7.1. To allow easy comparison between different discretizations, noting again that for each example  $N$  depends only on  $p$  (recall (7.1)), we denote the solution on the circles (with a slight abuse of notation) by  $u_p(t) := u_N(\mathbf{x}(t))$ ,  $t \in [0, 2\pi]$ , where  $t = 0$  corresponds to the direction from which  $u^i$  is incident. Plots of  $|u_7(t)|$  (i.e. the total field on the circle as computed with our finest discretization) for the equilateral triangle, for  $k = 10$  and  $k = 160$ , are shown in Figure 7.3. The shadow region and the regions in which specularly reflected waves are present are indicated (compare Figure 7.3 with Figure 7.1).

In Figure 7.4 we plot for both examples the relative maximum error on the circle,

$$\frac{\max_{t \in [0, 2\pi]} |u_7(t) - u_p(t)|}{\max_{t \in [0, 2\pi]} |u_7(t)|},$$

computed over 10000 evenly spaced points in  $[0, 2\pi]$ , for  $k = 10$ ,  $k = 40$ , and  $k = 160$ . The exponential decay with respect to increasing  $p$  predicted by Theorem 6.3 is clear for both examples (note the logarithmic scale on the vertical axes). Moreover, for fixed  $p$ , the relative maximum error seems to be, if anything, decreasing with increasing  $k$ , suggesting that the theoretical error bound (6.4) in Theorem 6.3 is not sharp in terms of its  $k$  dependence. As alluded to above, the errors in the domain are much

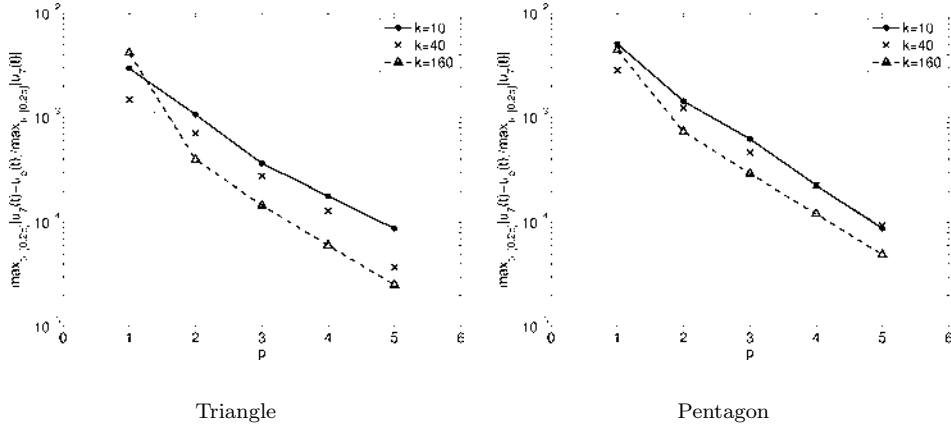


FIG. 7.4. Relative maximum errors on the circles of Figure 7.1.

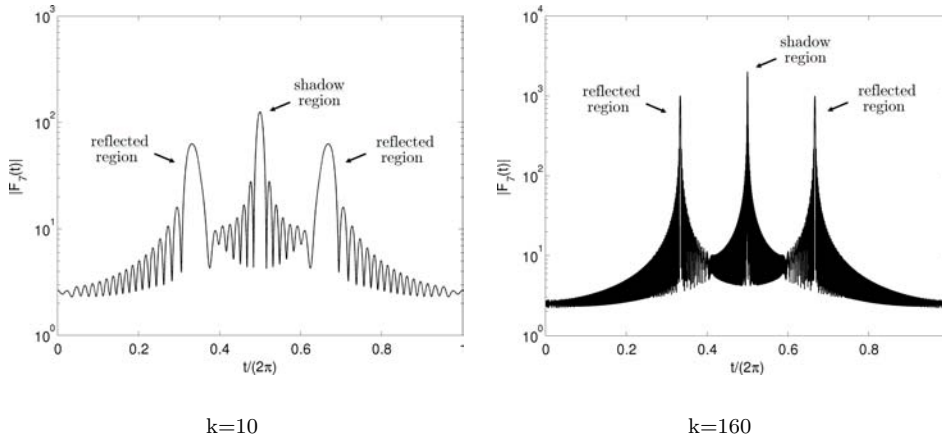


FIG. 7.5. Far field patterns for the triangle.

smaller than the relative errors in the computation of the boundary data in Figure 7.2, and, importantly, for fixed  $k$  and  $p$  the errors for the two examples are of similar magnitude. This suggests that the bound (6.4) in Theorem 6.3 is not sharp in terms of its dependence on the corner angles, either.

Finally, we compute our approximation to the far field pattern (6.7). As above, to allow easy comparison between different discretizations we denote (again with a slight abuse of notation)  $F_p(t) := F_N(\hat{\mathbf{x}}(t))$ ,  $t \in [0, 2\pi]$ , where  $t = 0$  again corresponds to the direction from which  $u^i$  is incident. Plots of  $|F_7(t)|$  (i.e. the far field pattern as computed with our finest discretization) for the triangle, for  $k = 10$  and  $k = 160$ , are shown in Figure 7.5. Again, the regions around the shadow and specularly-reflected directions are indicated.

In Figure 7.6 we plot approximations to  $\|F - F_N\|_{L^\infty(\mathbb{S}^1)}$  for  $k = 10$ ,  $k = 40$ , and  $k = 160$ , for both examples. To approximate the  $L^\infty$  norm, we compute both  $F_7$  and  $F_p$  at  $200k$  evenly spaced nodes on the unit circle. The exponential decay with

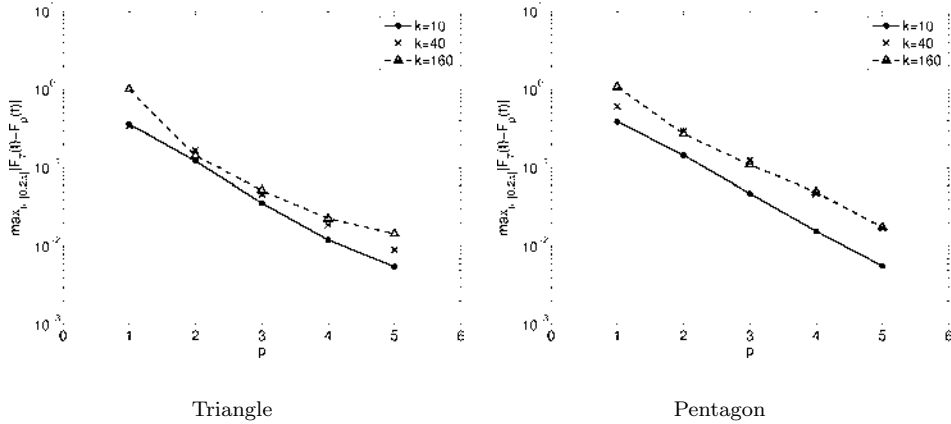


FIG. 7.6. Absolute maximum errors  $\|F_7 - F_p\|_{L^\infty(0,2\pi)}$  in the far field pattern.

respect to increasing  $p$  predicted by Theorem 6.4 is clear for both examples (note the logarithmic scale on the vertical axes). Moreover, for fixed  $p$ , the error does not grow significantly as  $k$  increases, indicating that, as for the solution in the domain, the  $k$  dependence of the bound (6.8) in Theorem 6.4 may not be optimal. Also, for fixed  $k$  and  $p$  the errors are comparable in magnitude for the two examples, suggesting that, as for the solution in the domain, the bound (6.8) may not be optimal in terms of its dependence on the corner angles, either.

In summary, our numerical examples demonstrate that the predicted exponential convergence of our  $hp$  scheme is achieved in practice. Moreover, for a fixed number of degrees of freedom, the accuracy of our numerical solution appears to deteriorate only very slowly (or not at all) as the wavenumber  $k$  increases. In fact, our results lead us to conjecture that *the theoretical error bounds provided by Corollary 6.2 and Theorems 6.3 and 6.4 are not sharp in their  $k$  dependence*. In particular, we believe that this is partly due to the lack of sharpness of our estimate for  $M$  derived in §4; indeed, we conjecture (cf. Remark 3.3) that  $M = \mathcal{O}(1)$  as  $k \rightarrow \infty$ , but, as yet, we do not have a proof of this result.

We also conjecture that *the theoretical error bounds provided by Theorems 6.3 and 6.4 are not sharp in their dependence on the corner angles of the polygon*. To explain this, we recall that our error estimates for the approximation of  $u$  by  $u_N$ , (6.4), and of  $F$  by  $F_N$ , (6.8), were derived via the Cauchy-Schwarz inequality and our  $L^2$  estimates for  $\varphi - \varphi_N$ , (6.2) and (6.3), which we know to blow up to infinity if one (or more) interior corner angle(s) tend to zero, reflecting that, in this limit,  $\varphi$  ceases to be in  $L^2(\Gamma)$ . Our choice of  $L^2(\Gamma)$  as the space for error analysis is motivated by the very recent results in [43], where coercivity was established with frequency independence for a second kind BIE formulation. One way to obtain error estimates which are uniform in the corner angles could be to work in a different function space, e.g.  $H^{-1/2}(\Gamma)$  or  $L^q(\Gamma)$  for  $q < 2$ , in which the norm of the boundary solution is bounded uniformly with respect to the corner angles. In particular, in the case of  $L^1(\Gamma)$ , for which we have presented numerical results, a key step in modifying our



analysis would be to use the bounds

$$|u(\mathbf{x}) - u_N(\mathbf{x})| = k |S_k(\varphi - \varphi_N)(\mathbf{x})| \leq k \max_{\mathbf{y} \in \Gamma} |\Phi_k(\mathbf{x}, \mathbf{y})| \|\varphi - \varphi_N\|_{L^1(\Gamma)}, \quad \mathbf{x} \in D,$$

$$|F(\hat{\mathbf{x}}) - F_N(\hat{\mathbf{x}})| \leq k \|\varphi - \varphi_N\|_{L^1(\Gamma)}, \quad \hat{\mathbf{x}} \in \mathbb{S}^1,$$

instead of (6.5) and (6.9), respectively. We remark that the former bound could provide a sharper estimate in particular for the case when  $\mathbf{x}$  is not near  $\Gamma$ , since  $\max_{\mathbf{y} \in \Gamma} |\Phi_k(\mathbf{x}, \mathbf{y})| \rightarrow 0$  as  $\mathbf{x} \rightarrow \infty$ . However, in order to obtain a complete theory of the form presented here, appropriately modified versions of Lemma 2.1, Lemma 2.2 and Assumption 2.3 would also be required. We do not explore these issues further here, except to say that the difficulty in dealing with the singularities when the corner angles are sharp is unrelated to considerations regarding the oscillatory nature of the solution, which form the main focus of this paper.

**8. Acknowledgements.** The authors thank S. N. Chandler-Wilde for many helpful discussions and A. Twigger for assistance with computing numerical results.

#### REFERENCES

- [1] *Digital Library of Mathematical Functions*. National Institute of Standards and Technology, from <http://dlmf.nist.gov/>, release date: 2010-05-07.
- [2] S. ARDEN, S. N. CHANDLER-WILDE, AND S. LANGDON, *A collocation method for high-frequency scattering by convex polygons*, J. Comp. Appl. Math., 204 (2007), pp. 334–343.
- [3] A. ASHEIM AND D. HUYBRECHS, *Local solutions to high-frequency 2d scattering problems*, J. Comput. Phys., 229 (2010), pp. 5357 – 5372.
- [4] I. BABUŠKA, B. Q. GUO, AND E. P. STEPHAN, *On the exponential convergence of the h-p version for boundary element Galerkin methods on polygons*, Math. Methods Appl. Sci., 12 (1990), pp. 413–427.
- [5] I. BABUŠKA AND M. SURI, *The p and h-p versions of the finite element method, basic principles and properties*, SIAM Rev., 36 (1994), pp. 578–632.
- [6] T. BETCKE, S. N. CHANDLER-WILDE, I. G. GRAHAM, S. LANGDON, AND M. LINDNER, *Condition number estimates for combined potential boundary integral operators in acoustics and their boundary element discretisation*, Numer. Methods PDEs, 27 (2011), pp. 31–69.
- [7] T. BETCKE AND E. A. SPENCE, *Numerical estimation of coercivity constants for boundary integral operators in acoustic scattering*, SIAM J. Numer. Anal., 49 (2011), pp. 1572–1601.
- [8] O. P. BRUNO, C. A. GEUZAINÉ, J. A. MONRO JR., AND F. REITICH, *Prescribed error tolerances within fixed computational times for scattering problems of arbitrarily high frequency: the convex case*, Philos. Trans. R. Soc. Lond. Ser. A, 362 (2004), pp. 629–645.
- [9] O. P. BRUNO AND F. REITICH, *High order methods for high-frequency scattering applications*, in Modeling and Computations in Electromagnetics, H. Ammari, ed., vol. 59 of Lect. Notes Comput. Sci. Eng., Springer, 2007, pp. 129–164.
- [10] S. N. CHANDLER-WILDE AND I. G. GRAHAM, *Boundary integral methods in high frequency scattering*, in Highly Oscillatory Problems, B. Engquist, T. Fokas, E. Hairer, and A. Iserles, eds., vol. 366 of London Math. Soc. Lecture Note Ser., CUP, 2009, pp. 154–193.
- [11] S. N. CHANDLER-WILDE, I. G. GRAHAM, S. LANGDON, AND M. LINDNER, *Condition number estimates for combined potential boundary integral operators in acoustic scattering*, J. Integral Equations Appl., 21 (2009), pp. 229–279.
- [12] S. N. CHANDLER-WILDE, I. G. GRAHAM, S. LANGDON, AND E. A. SPENCE, *Asymptotic-numerical boundary integral methods in high frequency acoustic scattering*, Acta Numer., (to appear 2012).
- [13] S. N. CHANDLER-WILDE, D. P. HEWETT, S. LANGDON, AND A. TWIGGER, *A high frequency boundary element method for scattering by a class of non-convex obstacles*. In preparation.
- [14] ———, *A high frequency BEM for scattering by non-convex obstacles*, in Proc. 10th Int. Conf. on Mathematical and Numerical Aspects of Waves, Vancouver, Canada, 2011, pp. 307–310.
- [15] S. N. CHANDLER-WILDE AND S. LANGDON, *A Galerkin boundary element method for high frequency scattering by convex polygons*, SIAM J. Numer. Anal., 45 (2007), pp. 610–640.
- [16] S. N. CHANDLER-WILDE, S. LANGDON, AND M. MOKGOLELE, *A high frequency boundary element*

- method for scattering by convex polygons with impedance boundary conditions, *Commun. Comput. Phys.*, 11 (2012), pp. 575–593.
- [17] S. N. CHANDLER-WILDE AND P. MONK, *Wave-number-explicit bounds in time-harmonic scattering*, *SIAM J. Math. Anal.*, 39 (2008), pp. 1428–1455.
- [18] D. COLTON AND R. KRESS, *Inverse Acoustic and Electromagnetic Scattering Theory*, Springer-Verlag, Berlin, 1992.
- [19] D. L. COLTON AND R. KRESS, *Integral equation methods in scattering theory*, John Wiley & Sons Inc., New York, 1983.
- [20] C. P. DAVIS AND W. C. CHEW, *Frequency-independent scattering from a flat strip with  $TE_z$ -polarized fields*, *IEEE Trans. Ant. Prop.*, 56 (2008), pp. 1008–1016.
- [21] V. DOMINGUEZ, I. G. GRAHAM, AND V. P. SMYSHLYAEV, *A hybrid numerical-asymptotic boundary integral method for high-frequency acoustic scattering*, *Numer. Math.*, 106 (2007), pp. 471–510.
- [22] M. GANESH AND S. C. HAWKINS, *A fully discrete Galerkin method for high frequency exterior acoustic scattering in three dimensions*, *J. Comput. Phys.*, 230 (2011), pp. 104–125.
- [23] W. GUI AND I. BABUŠKA, *The  $h$ -,  $p$ - and  $hp$ -versions of the finite element method in 1 dimension, parts I, II, III*, *Numer. Math.*, 49 (1986), pp. 577–683.
- [24] B. Q. GUO AND I. BABUŠKA, *The  $hp$ -version of the finite element method i. the basic approximation results and ii. general results and applications*, *Comp. Mech.*, 1 (1986), pp. 21–41 and 203–226.
- [25] N. HEUER, M. MAISCHAK, AND E. P. STEPHAN, *Exponential convergence of the  $hp$ -version for the boundary element method on open surfaces*, *Numer. Math.*, 83 (1999), pp. 641–666.
- [26] D. HUYBRECHS AND S. VANDEWALLE, *A sparse discretization for integral equation formulations of high frequency scattering problems*, *SIAM J. Sci. Comput.*, 29 (2007), pp. 2305–2328.
- [27] R. KRESS, *Linear Integral Equations*, Springer-Verlag, New York, 2nd ed., 1999.
- [28] S. LANGDON AND S. N. CHANDLER-WILDE, *A wavenumber independent boundary element method for an acoustic scattering problem*, *SIAM J. Numer. Anal.*, 43 (2006), pp. 2450–2477.
- [29] S. LANGDON, M. MOKGOLELE, AND S. N. CHANDLER-WILDE, *High frequency scattering by convex curvilinear polygons*, *J. Comput. Appl. Math.*, 234 (2010), pp. 2020–2026.
- [30] M. LÖHNDORF AND J. M. MELENK, *Wavenumber-explicit  $hp$ -BEM for high frequency scattering*, *SIAM J. Numer. Anal.*, 49 (2011), pp. 2340–2363.
- [31] T. LUOSTARI, T. HUTTUNEN, AND P. MONK, *Plane wave methods for approximating the time harmonic wave equation*, in *Highly Oscillatory Problems*, B. Engquist, T. Fokas, E. Hairer, and A. Iserles, eds., vol. 366 of *London Math. Soc. Lecture Note Ser.*, CUP, 2009, pp. 127–153.
- [32] M. MAISCHAK AND E. P. STEPHAN, *The  $hp$ -version of the boundary element method in  $\mathbb{R}^3$ : the basic approximation results*, *Math. Methods Appl. Sci.*, 20 (1997), pp. 461–476.
- [33] W. MCLEAN, *Strongly Elliptic Systems and Boundary Integral Equations*, CUP, 2000.
- [34] J. M. MELENK,  *$hp$ -Finite Element Methods for Singular Perturbations*, Springer, 2003.
- [35] J. M. MELENK AND S. LANGDON, *A fully discrete  $hp$  boundary element method for high frequency scattering by convex polygons*. In preparation.
- [36] ———, *An  $hp$ -boundary element method for high frequency scattering by convex polygons*, in *Proc. 8th Int. Conf. on Mathematical and Numerical Aspects of Waves*, Reading, UK, 2007, pp. 93–95.
- [37] J. M. MELENK AND S. SAUTER, *Wavenumber explicit convergence analysis for Galerkin discretizations of the Helmholtz equation*, *SIAM J. Numer. Anal.*, 49 (2011), pp. 1210–1243.
- [38] F. OBERHETTINGER AND L. BADI, *Tables of Laplace Transforms*, Springer-Verlag, 1973.
- [39] S. A. SAUTER AND C. SCHWAB, *Quadrature for  $hp$ -Galerkin BEM in  $\mathbf{R}^3$* , *Numer. Math.*, 78 (1997), pp. 211–258.
- [40] ———, *Boundary element methods*, vol. 39 of *Springer Series in Computational Mathematics*, Springer-Verlag, Berlin, 2011. Translated and expanded from the 2004 German original.
- [41] K. SCHERER, *On optimal global error bounds obtained by scaled local error estimates*, *Numer. Math.*, 36 (1981), pp. 151–176.
- [42] C. SCHWAB,  *$p$ - and  $hp$ -Finite Element Methods*, Clarendon Press, Oxford, 1998.
- [43] E. A. SPENCE, S. N. CHANDLER-WILDE, I. G. GRAHAM, AND V. P. SMYSHLYAEV, *A new frequency-uniform coercive boundary integral equation for acoustic scattering*, *Comm. Pure Appl. Math.*, 64 (2011), pp. 1384–1415.
- [44] F. STENGER, *Numerical Methods Based on Sinc and Analytic Functions*, Springer-Verlag, 1993.
- [45] E. P. STEPHAN, *The  $h$ - $p$  boundary element method for solving 2- and 3-dimensional problems*, *Comput. Methods Appl. Mech. Engrg.*, 133 (1996), pp. 183–208.
- [46] G. N. WATSON, *A Treatise on the Theory of Bessel Functions*, CUP, 2nd ed., 1944.

**Appendix A.  $hp$  Approximation Theory for Analytic Functions.**

In this section we present further details of the  $hp$ -approximation theory used in §5. We first note the following classical approximation result, which follows from [44, Theorem 2.1.1].

DEFINITION A.1. *Given  $-\infty < a < b < \infty$  and  $r > b - a$  define*

$$\mathcal{E}_{a,b,r} := \{w \in \mathbb{C} : |w - a| + |w - b| < r\}, \quad (\text{A.1})$$

which is the interior of an ellipse with foci  $\{a, b\}$ .

LEMMA A.2. *Suppose that a function  $g$  is analytic and bounded in  $\mathcal{E}_{a,b,r'}$  for some  $-\infty < a < b < \infty$  and  $r' > b - a$ . Then for  $b - a < r < r'$  we have the estimate*

$$\inf_{v \in \mathcal{P}_p(a,b)} \|g - v\|_{L^\infty(a,b)} \leq \frac{2}{\rho - 1} \rho^{-p} \|g\|_{L^\infty(\mathcal{E}_{a,b,r})}, \quad (\text{A.2})$$

where

$$\rho = \frac{1}{b - a} \left( r + \sqrt{r^2 - (b - a)^2} \right) > 1. \quad (\text{A.3})$$

Using this result we can prove Theorem 5.2.

*Proof.* (Proof of Theorem 5.2.) Part (ii) is clearly a trivial consequence of part (i). To prove (i), it is convenient to introduce the notation

$$E_i := \inf_{v \in \mathcal{P}_p(x_{i-1}, x_i)} \|g - v\|_{L^\infty(x_{i-1}, x_i)}, \quad (\text{A.4})$$

$$I_i := \inf_{v \in \mathcal{P}_p(x_{i-1}, x_i)} \|g - v\|_{L^2(x_{i-1}, x_i)}, \quad (\text{A.5})$$

for each  $i = 1, 2, \dots, n$ . We then have

$$\inf_{v \in \mathcal{P}_{p,n}(0,A)} \|g - v\|_{L^2(0,A)} = \left( \sum_{i=1}^n I_i^2 \right)^{1/2}, \quad (\text{A.6})$$

and to prove (i) we proceed to estimate  $I_i$  for each  $i = 1, \dots, n$  separately. We would like to use Lemma A.2 for this purpose, but for  $I_1$  this is not possible since around  $[x_0, x_1]$  we do not have the required ellipse of analyticity. However, crudely approximating by zero gives

$$I_1^2 \leq \int_0^{x_1} |g(x)|^2 dx \leq \hat{C}^2 \int_0^{x_1} x^{-2\delta} dx = \frac{\hat{C}^2 (A\sigma^{n-1})^{1-2\delta}}{1 - 2\delta} = \hat{C}^2 D_1 A^{1-2\delta} e^{-2n\vartheta}, \quad (\text{A.7})$$

where

$$\vartheta := |\log \sigma| (1/2 - \delta) > 0, \quad (\text{A.8})$$

and

$$D_1(\sigma, \delta) := \frac{\sigma^{2\delta-1}}{1 - 2\delta}. \quad (\text{A.9})$$

If  $n \geq 2$ , then for  $i = 2, 3, \dots, n$ ,  $g$  is analytic and bounded in the half plane  $\text{Re}[z] > \frac{x_i-1}{2}$ . With reference to Figure A.1, we note that for the general ellipse  $\mathcal{E}_{a,b,r}$

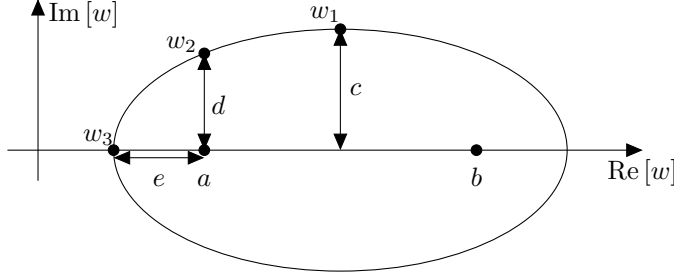


FIG. A.1. *Ellipse parameters.*

of Definition A.1, setting  $w = w_3$  reveals that  $r = 2e + (b - a)$ . Hence the largest ellipse  $\mathcal{E}_{x_{i-1}, x_i, r_i}$  lying inside the half-plane  $\text{Re}[z] > \frac{x_{i-1}}{2}$  has  $r_i = (x_i - x_{i-1}) + x_{i-1} = x_i$ . In fact,  $g$  is analytic and bounded in the bigger ellipse  $\mathcal{E}_{x_{i-1}, x_i, r'}$  for any  $r_i < r' < x_i + x_{i-1}$ , and so Lemma A.2 implies that

$$E_i \leq \frac{2B_i}{\rho_\sigma - 1} \rho_\sigma^{-p}, \quad i = 2, 3, \dots, n, \quad (\text{A.10})$$

where  $B_i := \|g\|_{L^\infty(\mathcal{E}_{x_{i-1}, x_i, r_i})}$  and

$$\rho_\sigma := \frac{1}{x_i - x_{i-1}} \left( r_i + \sqrt{r_i^2 - (x_i - x_{i-1})^2} \right) = \frac{1}{1 - \sigma} (1 + \sqrt{\sigma} \sqrt{2 - \sigma}) > 1. \quad (\text{A.11})$$

Hence

$$I_i^2 \leq \frac{4B_i^2 (x_i - x_{i-1})}{(\rho_\sigma - 1)^2} \rho_\sigma^{-2p}, \quad i = 2, 3, \dots, n. \quad (\text{A.12})$$

Now define  $n_*$  to be the largest  $i \in \{1, \dots, n\}$  such that  $\frac{x_{i-1}}{2} < 1$ , i.e.

$$n_* := \begin{cases} \left\lceil n - \left( \frac{\log A - \log 2}{|\log \sigma|} \right) \right\rceil, & \sigma A/2 \geq 1, \\ n, & \text{otherwise.} \end{cases} \quad (\text{A.13})$$

Then

$$B_i \leq \begin{cases} \hat{C} \left( \frac{x_{i-1}}{2} \right)^{-\delta} = \hat{C} \left( \frac{\sigma^{n-i+1} A}{2} \right)^{-\delta}, & 2 \leq i \leq n_*, \\ \hat{C} \left( \frac{x_{i-1}}{2} \right)^{-1/2} = \hat{C} \left( \frac{\sigma^{n-i+1} A}{2} \right)^{-1/2}, & n_* + 1 \leq i \leq n. \end{cases} \quad (\text{A.14})$$

Hence if  $n_* \geq 2$ , then for  $i = 2, \dots, n_*$  we have

$$B_i^2 (x_i - x_{i-1}) \leq \hat{C}^2 \left( \frac{\sigma^{n-i+1} A}{2} \right)^{-2\delta} \sigma^{n-i} A (1 - \sigma) = \frac{2^{2\delta} \hat{C}^2 (\sigma^{n-i} A)^{1-2\delta} (1 - \sigma)}{\sigma^{2\delta}}, \quad (\text{A.15})$$

so that

$$I_i^2 \leq \frac{2^{2+2\delta} \hat{C}^2 (\sigma^{n-i} A)^{1-2\delta} (1 - \sigma)}{\sigma^{2\delta} (\rho_\sigma - 1)^2} \rho_\sigma^{-2p}, \quad i = 2, \dots, n_*. \quad (\text{A.16})$$

By the definition of  $n_*$ ,  $\frac{x_{n_*-1}}{2} = \frac{A\sigma^{n-n_*+1}}{2} < 1$ , so  $\sigma^{n-i}A = \sigma^{n-n_*-1}A\sigma^{n_*+1-i} < 2\sigma^{-2}\sigma^{n_*+1-i}$ , and

$$\sum_{i=2}^{n_*} (\sigma^{n-i}A)^{1-2\delta} \leq (2\sigma^{-2})^{1-2\delta} \sum_{i=2}^{n_*} e^{-2(n_*+1-i)\vartheta} \leq \frac{(2\sigma^{-2})^{1-2\delta} e^{-2\vartheta}}{1 - e^{-2\vartheta}}, \quad (\text{A.17})$$

with  $\vartheta$  defined as in (A.8). Hence

$$\sum_{i=2}^{n_*} I_i^2 \leq \hat{C}^2 D_2 \rho_\sigma^{-2p}, \quad (\text{A.18})$$

where

$$D_2(\sigma, \delta) = \frac{2^{2+2\delta}(2\sigma^{-2})^{1-2\delta} e^{-2\vartheta} (1-\sigma)}{(1 - e^{-2\vartheta})\sigma^{2\delta}(\rho_\sigma - 1)^2} = \frac{8\sigma^{-1-4\delta}(1-\sigma)}{(1 - \sigma^{1-2\delta})(\rho_\sigma - 1)^2}. \quad (\text{A.19})$$

If  $n_* \leq n-1$  (i.e.  $\sigma A/2 \geq 1$ ), then for  $i = n_*+1, \dots, n$  we have the simpler result

$$B_i^2(x_i - x_{i-1}) = \hat{C}^2 \left( \frac{\sigma^{n-i+1}A}{2} \right)^{-1} \sigma^{n-i}A(1-\sigma) = \frac{2\hat{C}^2(1-\sigma)}{\sigma}, \quad (\text{A.20})$$

so that

$$I_i^2 \leq \frac{8\hat{C}^2(1-\sigma)}{\sigma(\rho_\sigma - 1)^2} \rho_\sigma^{-2p}, \quad i = n_*+1, \dots, n. \quad (\text{A.21})$$

Hence

$$\sum_{i=n_*+1}^n I_i^2 \leq (n - n_*)\hat{C}^2 D_3 \rho_\sigma^{-2p}, \quad (\text{A.22})$$

where

$$D_3(\sigma) = \frac{8(1-\sigma)}{\sigma(\rho_\sigma - 1)^2}. \quad (\text{A.23})$$

Note also that since  $\sigma A/2 \geq 1$  in this case, we can bound

$$n - n_* \leq \frac{\log A - \log 2}{|\log \sigma|} \leq \frac{\log A}{|\log \sigma|} \leq \frac{\log(2+A)}{|\log \sigma|}. \quad (\text{A.24})$$

Bring together the estimates (A.7), (A.18), (A.22) and (A.24), and noting that  $1 \leq 2 \log(2+A)$  for all  $A > 0$ , we obtain

$$\sum_{i=1}^n I_i^2 \leq \hat{C}^2 D_4 (A^{1-2\delta} e^{-2n\vartheta} + \log(2+A) e^{-2p\xi}), \quad (\text{A.25})$$

where  $\xi := \log \rho_\sigma > 0$ , and

$$D_4 = \max \left\{ D_1, 2D_2, \frac{D_3}{|\log \sigma|} \right\}. \quad (\text{A.26})$$

Recalling (A.6), the bound (5.7) then follows immediately with  $C = \sqrt{D_4}$ .  $\square$

Theorem 5.2 assumes the same polynomial degree on each element. In Remark 5.3 we claimed that one can reduce the total number of degrees of freedom, whilst maintaining exponential convergence as the maximum polynomial degree tends to infinity, by relaxing the assumption (5.4) and using a lower degree approximation near the singularity. Specifically, we have:

**THEOREM A.3.** *Suppose that the function  $g(z)$  satisfies the assumptions of Theorem 5.2. Given  $A > 0$ , and integers  $n \geq 1$  and  $p \geq 1$ , define a degree vector  $\mathbf{p}$  by*

$$(\mathbf{p})_i := \begin{cases} \left\lceil \frac{i-1}{n_*} p \right\rceil, & 1 \leq i \leq n_*, \\ p, & n_* + 1 \leq i \leq n, \end{cases}$$

where  $n_*$  is the largest  $i \in \{1, \dots, n\}$  such that  $\frac{x_{i-1}}{2} < 1$ , and  $x_i$  is defined as in Definition 5.1. Then

(i) *there exists a constant  $C' > 0$ , depending only on  $\delta$  and  $\sigma$ , such that the best  $L^2$  approximation error in  $\mathcal{P}_{\mathbf{p},n}(0, A)$  satisfies*

$$\inf_{v \in \mathcal{P}_{\mathbf{p},n}(0,A)} \|g - v\|_{L^2(0,A)} \leq C' \hat{C} \left( A^{1/2-\delta} e^{-n\vartheta} + (2+A)^{1/|\log \sigma|} e^{-n\nu} + \log^{1/2}(2+A) e^{-p\xi} \right), \quad (\text{A.27})$$

where  $\vartheta$  and  $\xi$  are as defined in Theorem 5.2, and  $\nu = \min \{\vartheta/2, p \log \rho_\sigma / n_*\}$ ;

(ii) *furthermore, if  $n$  is chosen such that  $cp \leq n \leq c'p$  for some constant  $c > 0$ , then*

$$\inf_{v \in \mathcal{P}_{\mathbf{p},n}(0,A)} \|g - v\|_{L^2(0,A)} \leq C' \hat{C} \left( A^{1/2-\delta} + (2+A)^{1/|\log \sigma|} + \log^{1/2}(2+A) \right) e^{-p\tau}, \quad (\text{A.28})$$

where  $\tau = \min \{c\vartheta/2, c \log \rho_\sigma / c', \xi\} > 0$ .

*Proof.* We proceed as per the proof of Theorem 5.2, except that if  $n_* \geq 2$  then for  $i = 2, \dots, n_*$  we must modify (A.16) by replacing  $p$  by  $(\mathbf{p})_i$ . Accordingly, instead of estimating the sum in (A.17), we must estimate

$$\sum_{i=2}^{n_*} (\sigma^{n-i} A)^{1-2\delta} \rho_\sigma^{-2(\mathbf{p})_i} \leq (2\sigma^{-2})^{1-2\delta} \sum_{i=2}^{n_*} e^{-(2(n_*+1-i)\vartheta + 2(i-1)\mu)}, \quad (\text{A.29})$$

where  $\mu := \frac{p \log \rho_\sigma}{n_*}$ . To do this, we write

$$2(n_* + 1 - i)\vartheta + 2(i - 1)\mu = (n_* + 1 - i)\vartheta + 2n_*\psi(i), \quad (\text{A.30})$$

where  $\psi(i) := \frac{1}{n_*} \left( (n_* + 1 - i)\frac{\vartheta}{2} + (i - 1)\mu \right)$ . Since  $\psi(i)$  is affine, we have

$$\psi(i) \geq \min \{\psi(1), \psi(n_* + 1)\} = \min \left\{ \frac{\vartheta}{2}, \mu \right\} =: \nu, \quad (\text{A.31})$$

which gives

$$\begin{aligned} \sum_{i=2}^{n_*} (\sigma^{n-i} A)^{1-2\delta} \rho_\sigma^{-2(\mathbf{p})_i} &\leq (2\sigma^{-2})^{1-2\delta} e^{-2n_*\nu} \sum_{i=2}^{n_*} e^{-(n_*+1-i)\vartheta} \\ &\leq (2\sigma^{-2})^{1-2\delta} \frac{e^{-\vartheta}}{1 - e^{-\vartheta}} e^{-2n_*\nu}, \end{aligned} \quad (\text{A.32})$$

so that

$$\sum_{i=2}^{n_*} I_i^2 \leq \hat{C}^2 D'_2 e^{-2n_*\nu}, \quad (\text{A.33})$$

where

$$D'_2(\sigma, \delta) = \frac{8\sigma^{-3/2-3\delta}(1-\sigma)}{(1-\sigma^{1/2-\delta})(\rho_\sigma-1)^2}. \quad (\text{A.34})$$

The bound (A.25) is then replaced by

$$\sum_{i=1}^n I_i^2 \leq \hat{C}^2 D'_4 (A^{1-2\delta} e^{-2n\vartheta} + e^{-2n_*\nu} + \log(2+A)e^{-2p\xi}), \quad (\text{A.35})$$

where

$$D'_4 = \max \left\{ D_1, D'_2, \frac{D_3}{|\log \sigma|} \right\}, \quad (\text{A.36})$$

giving

$$\inf_{v \in \tilde{\mathcal{P}}_{\mathbf{p}, n}(0, A)} \|g - v\|_{L^2(0, A)} \leq C' \hat{C} \left( A^{1/2-\delta} e^{-n\vartheta} + e^{-n_*\nu} + \log^{1/2}(2+A)e^{-p\xi} \right), \quad (\text{A.37})$$

where  $C' := \sqrt{D'_4}$ . Finally, we obtain (A.27) by noting that

$$n_* \geq n - \frac{\log(2+A)}{|\log \sigma|}, \quad (\text{A.38})$$

which follows from (A.24) for  $\sigma A/2 \geq 1$  and the fact that  $n_* = n$  for  $\sigma A/2 < 1$ .

Part (ii) follows trivially from part (i). The restriction that  $n$  be bounded above as well as below in terms of  $p$  is needed to ensure that  $\tau$ , which depends on  $p$  and  $n_*$  through  $\mu$ , is bounded away from zero, so that (A.28) represents exponential decay as  $p \rightarrow \infty$ . Recalling that  $\mu = p \log \rho_\sigma / n_*$ , we must ensure that  $p/n_*$  is bounded away from zero. But since  $n_* \leq n \leq c'p$ , we have  $p/n_* \geq 1/c' > 0$ .  $\square$